EXHIBIT A

The EMBO Journal vol.6 no.1 pp.187–193, 1987

Translational efficiency of polycistronic mRNAs and their utilization to express heterologous genes in mammalian cells

Randal J.Kaufman, Patricia Murtha and Monique V.Davies

Genetics Institute, Cambridge, MA 02140, USA

Communicated by J.Tata

The translation of polycistronic mRNAs in mammalian cells was studied. Transcription units, constructed to contain one, two or three open reading frames (ORFs), were introduced stably into Chinese hamster ovary cells and transiently into COS monkey cells. The analysis of mRNA levels and protein synthesis in these cells demonstrated that the mRNAs transcribed were translated to generate multiple proteins. The efficiency of translation was reduced ~40- to 300-fold by the insertion of an upstream ORF. The results support a modified 'scanning' model for translation initiation which allows for translation initiation at internal AUG codons. High-level expression of human granulocyte–macrophage colony stimulating factor was achieved utilizing a vector that contains a polycistronic transcription unit encoding an amplifiable dihydrofolate reductase marker gene in its 3′ end. Thus, polycistronic expression vectors can be exploited to obtain high-level expression of foreign genes in mammalian cells.

Key words: polycistronic transcription unit/gene expression/gene transfer/expression vectors

Introduction

Although the precise mechanism by which eukaryotic ribosomes recognize particular initiation sites in mRNA molecules is unclear, a substantial amount of evidence supports a 'scanning' model for translation initiation (Kozak, 1980a). This model suggests that a 40S ribosomal subunit binds to the 5′ capped end of the mRNA and migrates in the 3′ direction until it encounters the first AUG triplet which, if present in an appropriate context, can efficiently serve as the initiator codon. The scanning model is supported by the stimulatory effect of the m^7G cap (Shatkin, 1976), the inability of ribosomes to bind circular mRNAs (Kozak, 1979a; Konarska *et al.*, 1981), the ability of 40S subunits to migrate along the mRNA (Kozak and Shatkin, 1978; Kozak, 1979b, 1980b), and the negative influence of significant secondary structure and of additional AUGs inserted between the 5′ end of the mRNA and the initiation codon (Kozak, 1984, 1986; Liu *et al.*, 1984; Pelletier and Sonnenberg, 1985). The finding that eukaryotic ribosomes usually translate only from the 5′ proximal AUG in polycistronic mRNAs is also supportive of a scanning model. However, many naturally occurring mRNAs are known to initiate at internal AUGs (Ghosh *et al.*, 1978; Wengler *et al.*, 1979; Perler *et al.*, 1980; Bos *et al.*, 1981; Hagenbuchle *et al.*, 1981; Hendy *et al.*, 1981; Vogeli *et al.*, 1981; Clerx-van Haaster *et al.*, 1982; Swanström *et al.*, 1982; Yoo *et al.*, 1982; Marsden *et al.*, 1983; Hughes *et al.*, 1984; Dixon and Hohn, 1984). In addition, several studies have demonstrated translation initiation from internal AUG codons in experimental constructs, by the insertion or deletion of initiator or terminator codons upstream from the translation start site of a particular open reading frame (ORF) (Dixon and Hohn, 1984; Hughes *et al.*, 1983; Kozak, 1984; Liu *et al.*, 1984). These studies demonstrate that the insertion of an upstream AUG, which is out of frame with the downstream ORF, can severely suppress translation of the downstream ORF. Insertion of a termination codon can reverse the suppression. Thus, these studies suggest a modified scanning model with the potential for reinitiation at internal, downstream AUGs. However, to date there have been few reports that polycistronic mRNAs can actually translate two or more proteins from non-overlapping ORFs in the same transcription unit in mammalian cells (Mertz *et al.*, 1983; Herman, 1986; Peabody *et al.*, 1986; Peabody and Berg, 1986).

We have examined the translational efficiency of polycistronic mRNAs in mammalian cells. Plasmids harboring transcription units constructed to contain one, two or three ORFs encoding protein products that can be easily monitored, were introduced into Chinese hamster ovary (CHO) cells by stable transformation or into COS monkey cells by transient transfection. The results demonstrate that both cell types are capable of translating multiple non-overlapping ORFs from a single polycistronic transcript. However, the efficiency of translation from an ORF was dramatically reduced by the presence of upstream ORFs. Direct selection for the gene product encoded from the 3′ proximal ORF is demonstrated to provide a useful means to obtain expression of heterologous genes in mammalian cells.

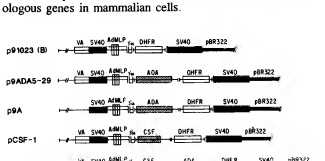

Fig. 1. Structure of polycistronic expression vectors. The derivation of these vectors is described in Materials and methods. The functional elements of the expression vectors are depicted and have been described previously (Kaufman and Sharp, 1982a,b). All vectors utilize the adenovirus major late promoter for transcription initiation and contain the majority of the adenovirus tripartite leader present on adenovirus late mRNAs. A small intron is present consisting of a 5′ splice site from the adenovirus first late leader and an introduced 3′ splice site. In addition the vectors contain the SV40 origin of replication and transcriptional enhancer, and the SV40 early polyadenylation signal. Four of the vectors contain the adenovirus VA genes (VA) as shown. All vectors are contained in a derivative of pSVOd (Mellon *et al.*, 1981). The murine DHFR, murine ADA and human GM-CSF (CSF) coding regions are represented. The 3′ untranslated region of GM-CSF is 330 bases and contains an ORF of 273 bases. The 3′ untranslated region of ADA is 147 bases and contains a short ORF of 18 bases. The 5′ untranslated region of DHFR is 105 bases, contains no AUGs and has an 18-bp poly(G) tail from the cDNA cloning (Kaufman and Sharp, 1982b). The 5′ untranslated region of ADA contains an *Eco*RI site (GAATTCATG) at the translation initiation site.

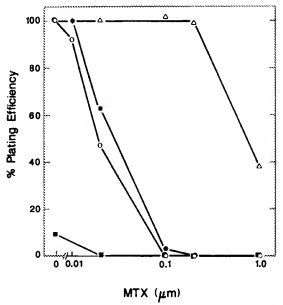

Fig. 2. Plating efficiency versus MTX concentration of ADA transformants before and after ADA amplification. The plating efficiency for an original ADA transformant (1−0.1, ■) grown in 0.1 μM 2′-deoxycoformycin and two amplified transformants (1−100, ○; and 2−100, ●) grown in 100 μM 2′-deoxycoformycin were determined by plating 200 and 2000 cells per 10-cm dish in nucleoside-free alpha media with increasing concentrations of MTX. Colonies were stained and counted 12 days after plating. Values are expressed as a per cent of the control (media containing 1.1 mM adenosine, 1 mM uridine, 10 μg/ml deoxyadenosine, 110 μg/ml thymidine, and without 2′-deoxycoformycin and MTX) which was 23% for the clone 1−0.1, 30% for the clone 2−0.1 and 22% for the clone 1−100. Also shown is the plating efficiency of clone E6−0.1, which is a cell line selected for growth in 0.1 μM MTX as a result of expression from p91023(B) (△).

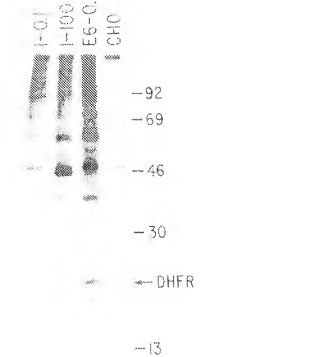

Fig. 3. Analysis of DHFR synthesis in ADA amplified and control CHO cells. Cells were labeled for 45 min with [35S]methionine and cell extracts prepared for immunoprecipitation as described by Kaufman *et al.* (1985) with a rabbit anti-DHFR antibody. The cell lines indicated are clone 1 in 0.1 μM (1−0.1) and 100 μM (1−100) 2′-deoxycoformycin, another CHO cell line resistant to 0.1 μM MTX after transfection with p91023(B) (E6−0.1), and the original CHO cells (CHO). The band migrating at 45-kd in the 1−100 cells is ADA.

Results

Translation of a dicistronic mRNA in stable transformed CHO cells

The potential of polycistronic mRNAs to generate multiple proteins from non-overlapping reading frames was studied by the construction of vectors to transcribe mRNAs encoding multiple ORFS (depicted in Figure 1), and analysis of the proteins expressed after their transient introduction into COS monkey cells, or stable introduction into CHO cells. p9ADA5-29 (Figure 1), which encodes a dicistronic adenosine deaminase−dihydrofolate reductase (ADA−DHFR) transcription unit, was introduced into DHFR-deficient CHO cells, and transformants isolated by selection for ADA expression (Kaufman *et al.*, 1986a). Two transformants were randomly chosen and propagated in increasing concentrations of 2′-deoxycoformycin, a tight-binding inhibitor of ADA. This selection resulted in cells which were resistant to 100 μM 2′-deoxycoformycin, and which contained ~500 copies of the plasmid DNA integrated into the CHO cell genome (Kaufman *et al.*, 1986a). These cells, which were initially DHFR-deficient, were then analysed for their level of DHFR expression. In order to monitor functional DHFR expression from the dicistronic transcription unit, the cells were grown under conditions that require functional DHFR, i.e. growth in the absence of added nucleosides. In addition, the growth potential as a function of increasing concentrations of methotrexate (MTX) was determined to provide an indication of the level of DHFR expression. Figure 2 shows the results of a plating efficiency experiment, where an original ADA transformant and two highly amplified clones were propagated in increasing concentrations of MTX. The result demonstrates that 8% of the population of the original transformant grew in the DHFR-selective media. The plating efficiency, in the DHFR-selective media, of the highly amplified cell line was 100%. As the MTX concentration was increased, the plating efficiency decreased, which is consistent with the growth observed being due to function DHFR expression. Low levels of MTX had little effect on the plating efficiency, whereas 0.2 μM reduced the plating efficiency to <1%. In contrast, a cell line selected for resistance to 0.1 μM MTX, by DHFR expression from a monocistronic transcription unit, was capable of growth in MTX concentrations up to 1.0 μM. These results demonstrate a low, but significant, level of DHFR expression from the ADA−DHFR dicistronic expression vector, in the absence of any direct selection for DHFR expression. Thus, it can be concluded that cells which have amplified the ADA−DHFR dicistronic transcription unit appear to express both ADA and DHFR proteins on the basis of the observed resistance of these cells to the appropriate selective agents.

DHFR protein synthesis was directly demonstrated by L[35S]methionine labeling of CHO cells transfected with p9ADA5-29, and immunoprecipitation with a rabbit anti-mouse DHFR antibody (Figure 3). A 20-kd band was found to comigrate with authentic murine DHFR (Figure 3, cell line 1−100).

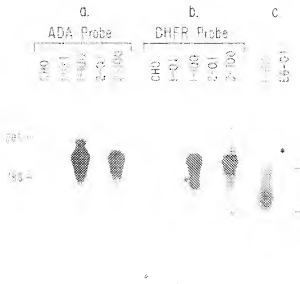

Fig. 4. RNA blot hybridization analysis of original and ADA amplified cell lines. Total RNA was isolated and electrophoresed on formaldehyde–formamide denaturing 1% agarose gels and transferred to nitrocellulose paper as described in Materials and methods. Hybridization as to a nick-translated probe from a fragment of the ADA coding region (**a**) or to the DHFR coding region (**b,c**). The filter represented in **panel a** was washed and rehybridized with the DHFR probe (**b**). The cell lines indicated are as described in Figure 2. Indicated are the 18S and 28S rRNA marker bands. The source or the band migrating below 28S in clone E6−0.1 is not known, but it does not appear in poly(A)-containing RNA.

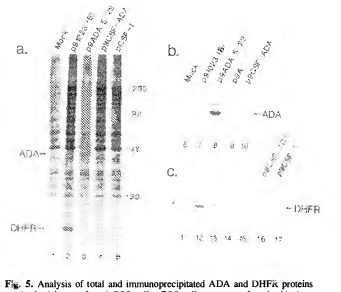

Fig. 5. Analysis of total and immunoprecipitated ADA and DHFR proteins synthesized in transfected COS cells. COS cells were transfected with the plasmids indicated as described in Materials and methods. Sixty hours post-transfection, the cells were labeled with [^{35}S]methionine for 1 h and cell extracts taken for anlaysis by SDS−reducing polyacrylamide gel electrophoresis before and after immunoprecipitation with either an anti-ADA antibody (**panel b**) or an anti-DHFR antibody (**panel c**). **Panel a** represents the total protein synthesis. Samples 6−10 correspond to samples 11−15, respectively. Samples 16 and 17 were obtained from a separate transfection. The lanes are labeled with the plasmid DNA which was transfected into the cells. Mock refers to cells which did not receive DNA. The bands migrating at 20 and 44 kd are DHFR and ADA as indicated. The band migrating above ADA in **lane 8** is also ADA. The band migrating slightly above the murine DHFR in **panel c** is the monkey DHFR. In order to guarantee quantitative immunoprecipitation, only 1/20 of the cell extract was immunoprecipitated for samples in **lanes 8, 9** and **12** compared with the other lanes. The conditions for the immunoprecipitation were determined by demonstrating that reprecipitation of immunoprecipitated supernatants did not bring down significantly more antigen. Samples 11, 13, 14 and 15 all exhibit similar amounts of endogenous monkey DHFR (*), again demonstrating quantitative immunoprecipitation.

The amount of this protein increased as the level of resistance to 2′-deoxycoformycin was increased: compare cell line 1−0.1, which was resistant to 0.1 μM with cell line 1−100, resistant to 100 μM. This increase is presumably due to amplification of the ADA− DHFR transcription unit in these cells (Kaufman *et al.*, 1986a). For reference, see the level of DHFR produced by the cell line E6−0.1, which has a monocistronic DHFR transcription unit, synthesizes several fold greater levels of DHFR, and is resistant to 0.1 μM MTX compared with line 1−100.

In order to confirm that the DHFR expression osberved was derived from the ADA−DHFR dicistronic mRNA, the cells were examined by DNA and RNA blot hybridization analysis. RNA blot hybridization analysis demonstrated the appearance of a single mRNA, using either ADA- or DHFR-specific hybridization probes, which had the size expected for the mRNA encoded by the dicistronic transcription unit (Figure 4). Comparison with the CHO cell line resistant to 0.1 μM MTX (E6−0.1 in Figure 3) as a result of expression from a monocistronic transcription unit, demonstrated the appearance of a 12-fold less abundant DHFR mRNA in clone E6−0.1 (Figure 4, panel c). Thus, DHFR expression at this level would generate a detectable transcript by this analysis. Comparison of the band intensities in order to quantitate DHFR protein levels in these lines indicated that DHFR synthesis in E6−0.1 is 3-fold greater than in 1−100. Comparison of the abundance of DHFR mRNA species in these two cell lines and of the relative amount of DHFR synthesis (Figures 3 and 4, panel c) indicates that the monocistronic mRNA translates DHFR ~36-fold more efficiently than the dicistronic mRNA derived from p9ADA5-29.

Southern blot analysis by hybridization to a probe specific to the 5′ end of the DHFR coding sequence indicated a single DHFR sequence had integrated and that no rearrangement of sequences surrounding the integrated DHFR DNA had occurred as a result of selection for ADA gene amplification (data not shown).

Translation of dicistronic and tricistronic mRNAs in transiently transfected COS monkey cells

The results from CHO cells indicate that dicistronic mRNAs can be translated, but the translation efficiency of the downstream ORF, in the construct tested, is dramatically reduced. In order to determine if the introduction of another ORF, upstream of DHFR, has further suppressive effects, an ORF encoding human granulocyte−macrophage colony stimulating factor (GM-CSF) was introduced 5′ of the ADA ORF to obtain p9CSF-ADA (Figure 1). In order to assay more conveniently for translation of the resultant polycistronic mRNAs, these plasmid DNAs were transiently introduced into COS monkey cells. Seventy-two hours post-transfection, the cells were labeled for 1 h with L[^{35}S]methionine and cell extracts prepared for immunoprecipitation and SDS−polyacrylamide gel electrophoresis (Figure 5). Cells transfected with p9CSF-ADA express ~1 μg GM-CSF/10^6 cells/day. Results demonstrate that DHFR and ADA represent a major proportion (~5%) of the total protein synthesis in cells transfected with p91023(b) and p9ADA5-29 respectively (Figure 5, panel a). DHFR synthesis could not be detected in cells transfected with p9ADA5-29 and p9CSF-ADA by analysis of total protein

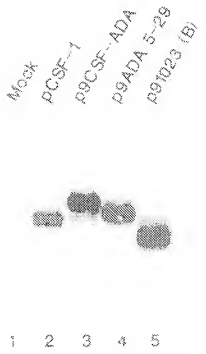

Fig. 6. RNA blot analysis of transfected COS cells. COS cells were transfected with the indicated plasmid as described in Materials and methods. Total RNA was harvested 60 h after transfection and electrophoresed and analysed by RNA blotting procedures as described in Materials and methods. Filters were hybridized to a DHFR cDNA probe prepared by nick-translation of a *Pst*I fragment isolated by gel electrophoresis. The expected sizes of the p91023(B), p9ADA5-29, p9CSF-ADA and pCSF-1 transcripts are 1150, 2290, 3060 and 1920 bases, respectively.

Table I. Summary of COS cell expression of ADA and DHFR from polycistronic transcripts

ORF order (plasmid)	Relative expression level	
	DHFR	ADA
DHFR [p91023(B)]	1	
CSF-DHFR (pCSF-1)	1/300	
ADA−DHFR (p9ADA5-29)	1/100	1
CSF-ADA−DHFR (p9CSF-ADA)	1/300	1/150

Relative levels of ADA and DHFR expression are indicated as quantitated from results shown in Figure 5 as described in Materials and methods.

synthesis on SDS−polyacrylamide gels (Figure 5, panel a). Analysis by immunoprecipitation with anti-DHFR and anti-ADA antibodies is shown in Figure 5 (panels b and c). In order to guarantee quantitative immunoprecipitation, lanes 8, 9 and 12 represent 1/20 of the cell extracts that were immunoprecipitated in the other lanes. Introduction of the ADA ORF, 5′ proximal to DHFR, resulted in a 100-fold decrease in translation of DHFR. Similarly, the introduction of CSF ORF to generate pCSF-1 resulted in a 300-fold decrease in DHFR translation. The introduction of the CSF ORF into p9ADA5-29 to generate p9CSF-ADA results in a 150-fold reduction in ADA translation (panel b, lane 10) when compared with the synthesis of ADA in p9ADA5-29 (panel b, lane 8) but only a 3-fold reduction in DHFR translation relative to p9ADA5-29 (panel c, lanes 13 and 15). Similarly, the introduction of the ADA ORF in between the GM-CSF and DHFR ORFs in pCSF-1 to generate p9CSF-ADA does not result in a decrease in DHFR translation (panel c, lanes 16 and 17). RNA blot analysis demonstrated that the plasmids direct the synthesis of equivalent amounts of single mRNAs of the expected size (Figure 6). Further hybridization analysis with ADA and GM-CSF labeled probes demonstrated that the observed mRNAs contain the expected ORFs (data not shown).

The results from these COS cell experiments are summarized in Table I. The results demonstrate the ability of cells to translate polycistronic mRNAs encoding GM-CSF, ADA and DHFR. However, there is a 100-fold reduction in DHFR translation, by insertion of an upstream ADA ORF, and only a further 3- to 4-fold reduction by the additional insertion of a GM-CSF ORF, 5′ of the DHFR ORF. Thus, the insertion of a single upstream ORF severely suppresses DHFR translation in COS cells, as was found in CHO cells. However, the insertion of an additional ORF has a smaller effect on DHFR translation.

Previous experiments have demonstrated the ability of adenovirus virus-associated (VA) RNA to potentiate translation in transiently transfected COS cells (Kaufman, 1985). The ability of VA RNA to potentiate the translation of polycistronic mRNAs is shown in Figure 5. Expression of DHFR from an ADA−DHFR dicistronic transcription unit contained in p9A (Figure 1) which has deleted the adenovirus VA genes is reduced by 10-fold (Figure 5, panel c, lanes 13 and 14), similar to the 8-fold reduction seen for ADA (Figure 5, panel b, lanes 8 and 9). The differences in ADA and DHFR expression in response to adenovirus VA RNA result from differences in translation, since the level of the dicistronic mRNA is not affected by the presence of VA RNA (data not shown). This result demonstrates that VA affects translation initiation at internal AUGs, in the same way as AUGs at the 5′ proximal end of the mRNA.

Utilization of polycistronic transcription units to efficiently express heterologous genes

The inefficient translation of ORFs present in the 3′ end of mRNAs can provide a unique approach to obtain high-level expression of heterologous genes in mammalian cells, by direct selection for expression of an inefficiently translated, amplifiable marker gene carried in the 3′ end of a particular transcription unit. This has been demonstrated by transformation of DHFR-deficient CHO cells with a plasmid which is capable of encoding GM-CSF and DHFR in a dicistronic transcription unit. The plasmid pCSF-1 was introduced into CHO DHFR-deficient cells by protoplast fusion and transformants selected directly for DHFR expression. A pool of DHFR-positive colonies was propagated in sequentially increasing concentrations of MTX. Analysis of GM-CSF activity indicated that as cells became increasingly resistant to MTX, the level of GM-CSF expression correspondingly increased. The comparison with cells derived by co-transfection of pCSF-1 with DHFR expression plasmids (as described by Kaufman *et al.*, 1985) indicated that selection for the polycistronic GM-CSF−DHFR alone yielded initial transformants which express ~10-fold higher levels of GM-CSF (data not shown).

Analysis of the level of CSF protein synthesis and secretion is shown in Figure 7. Cells selected for resistance to 2.0 μM and 100 μM MTX were labeled with [^{35}S]methionine for 1 h and conditioned media and cell extracts prepared and analysed by SDS−polyacrylamide gel electrophoresis. In comparison with the secreted, labeled proteins from the original DHFR-deficient CHO cells, a smear from 15 to 32 kd is observed in cells (clone D2) resistant to 2.0 μM MTX. These species are specifically immunoprecipitated with a rabbit anti-human GM-CSF antisera. The heterogeneity in mol. wt results from extensive glycosylation

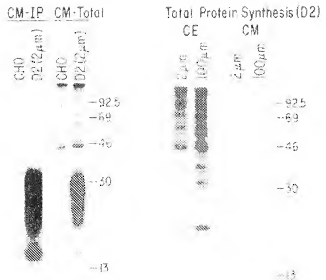

Fig. 7. Synthesis and secretion of human GM-CSF expressed in CHO cells. The GM-CSF producing CHO cell clone D2 resistant to 2 μM and 100 μM MTX was labeled with [^{35}S]methionine for 1 h and cell extracts (CE) and conditioned media (CM) taken for analysis by SDS–polyacrylamide gel electrophoresis before (**middle** and **right panels**) and after (**left panel**) immunoprecipitation with a rabbit anti-human GM-CSF antisera. Also shown is a control of the original CHO cells (CHO).

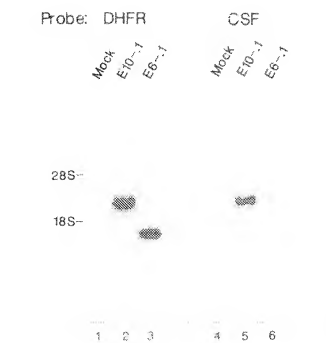

Fig. 8. RNA blot analysis of GM-CSF and DHFR mRNAs in GM-CSF producing CHO cells. Total RNA was isolated from the original CHO cells (mock), the GM-CSF producing pool E10 resistant to 0.1 μM MTX (E10–.1), and another CHO line resistant to 0.1 μM MTX by expression of a monocistronic DHFR transcript (E6–.1) and analysed by gel electrophoresis and RNA blotting procedures. Parallel RNA blots were hybridized to a DHFR probe or a GM-CSF probe prepared by nick-translation of isolated gel fragments.

of CSF and is similar to that observed from activated T cells (Wong *et al.*, 1985). GM-CSF represents the majority of protein secreted in the 2.0 μM MTX-resistant cells and >90% of the total protein secreted in the cells selected for resistance to 100 μM MTX. Upon selection for resistance to higher MTX, there is no apparent change in the nature or extent of glycosylation as monitored by this analysis. The band migrating at 20 kd in the cell extracts is DHFR.

Analysis of the mRNA and the DNA in the CHO cells transformed to the DHFR-positive phenotype with pCSF-1 and subsequently amplified by MTX resistance selection, demonstrated CSF and DHFR expression resulted from a dicistronic mRNA. Northern blot analysis indicated the presence of a single 1.8-kb mRNA, the expected size for the transcript (Figure 8). Southern blot analysis demonstrated a unique band which co-migrated the appropriate *Bam*HI fragment from pCSF-1 (data not shown). Since *Bam*HI sites flank the polycistronic transcription unit, the integrity of this fragment was not lost upon transfection and selection for amplification. The copy number in cells resistant to 2 μM MTX is ~2000 copies/cell. By comparison with previous reports (Lau *et al.*, 1984; Kaufman *et al.*, 1985, 1986b), this represents a very high degree of gene amplification at a relatively moderate level of MTX resistance. This high degree of amplification is probably a result of the inefficient expression of DHFR from the dicistronic transcript. The D2 cells resistant to 2 μM MTX contain one or two significant chromosomal homogeneously staining regions (HSRs) and the GM-CSF expression level has been maintained stably for over 1 year in culture in the presence of MTX (data not shown). These are characteristics typical of CHO cells containing high degrees of gene amplification (Kaufman *et al.*, 1983; Lau *et al.*, 1984). These results demonstrate that polycistronic transcription units can provide a convenient means to select cells which efficiently express heterologous genes.

Discussion

Transcription units have been constructed which contain multiple ORFs encoding DHFR, ADA and GM-CSF. The expression of these proteins from a single mRNA has been studied in stably transformed CHO cells and in transiently transfected COS monkey cells. Using a series of polycistronic expression vectors, the translational efficiency was shown to be dramatically reduced by insertion of upstream ORFs. The efficiency of DHFR translation decreased ~40- and 100-fold in CHO and COS cells, respectively, by the insertion of an upstream ADA ORF. Similarly, the 5′ insertion of a GM-CSF ORF, resulted in a 150- and a 300-fold decrease in ADA and DHFR translation, respectively, in the resultant dicistronic mRNAs. The 5′ insertion of the GM-CSF ORF into an ADA–DHFR dicistronic transcription unit resulted in a 150-fold decrease in ADA translation, but only a 3-fold decrease in DHFR translation. The dramatic decrease in DHFR translation by insertion of a single 5′ ORF is in contrast to the small decreases in DHFR translation observed from polycistronic mRNAs by Peabody *et al.* (1986). This may suggest that the primary nucleotide sequences, its length, or mRNA secondary structure may dramatically affect the frequency of internal translation initiation. The negative influence of upstream ORFs on translation initiation is consistent with previous work, which has shown that AUG codons, inserted upstream of the 'correct' AUG initiation codon, reduces translation at the 'correct' site (Dixon and Hohn, 1984; Hughes *et al.*, 1984; Kozak, 1984; Liu *et al.*, 1984). These results suggest that internal initiation occurs by translation reinitiation as opposed to independent in-

ternal initiation. However, results reported here demonstrate 5′ insertion of an ORF to generate a tricistronic mRNA dramatically reduces translation of the second ORF (150-fold) whereas translation of the third ORF is only slightly reduced (3-fold). A possible explanation for this finding is the occurrence of independent internal initiation at internal AUGs. However, our data cannot rule out other possibilities.

Previous studies have demonstrated inefficient translation of some mRNAs after transient transfection of plasmid DNA into cells (Svensson and Akusjarvi, 1984, 1985; Kaufman, 1985). The inefficiency in translation of these mRNAs can be corrected by the presence of adenovirus VA RNA. Although the role of VA RNA in potentiating translation in transfected cells has not been elucidated, its role has been intensively studied in adenovirus-infected cells (Reichel *et al.*, 1985; Kitajewski *et al.*, 1986; O'Malley *et al.*, 1986). These studies have demonstrated that VA RNA is likely to act by increasing the levels of functional eIF-2 by preventing phosphorylation of its alpha subunit through direct inhibition of the double-strand RNA-activated protein kinase (DAI kinase). Studies presented here have demonstrated the ability of VA equally to potentiate translation at internal and 5′ proximal AUGs. These results suggest that internal initiation, similar to initiation at the 5′ end of the mRNA, may be affected by altered levels of eIF-2.

DHFR has been useful as an amplifiable marker and has been exploited to obtain high-level expression of heterologous genes in mammalian cells (Haynes and Weissman, 1983; Scahill *et al.*, 1983; Lau *et al.*, 1984; McCormick *et al.*, 1984; Kaufman *et al.*, 1985, 1986b). However, co-transfection and co-amplification of a heterologous gene with a DHFR gene frequently results in deletion of the desired heterologous gene (Kaufman and Sharp, 1982a; Kaufman *et al.*, 1985). The use of polycistronic expression vectors, that encode transcripts containing the desired coding region upstream of the DHFR coding region, can provide an approach to solve this problem; the heterologous gene and the DHFR gene can be linked on the same transcription unit, and as a result the possibility of deletion may be reduced. The ability to select directly for DHFR expression from a GM-CSF and DHFR polycistronic transcription unit was demonstrated. Selection for cells which are moderately resistant to MTX resulted in cells which have a high level of GM-CSF−DHFR transcript, encoded by a highly amplified transcription unit.

The DHFR co-amplification approach to heterologous gene expression has generally been limited to CHO cells which are deficient in DHFR. The dicistronic ADA−DHFR vector described here provides a unique opportunity to introduce and amplify foreign genes to very high copy number in a variety of mammalian cells. First, since ADA can function as a dominant selectable and amplifiable marker for gene transfer in a variety of cells (Kaufman *et al.*, 1986a), initial transformants can be selected for ADA expression, and the DNA amplified by growth in increasing concentrations of 2′-deoxycoformycin. Second, cells selected to contain a high degree of amplification of the ADA−DHFR polycistronic transcription unit, should also produce a sufficient amount of DHFR to allow MTX resistance selection in order to amplify further the gene copy number. The potential usefulness of this doubly amplifiable vector is currently being evaluated.

Materials and methods

Vector construction

Figure 1 depicts the functional components of the expression plasmids used in this study. The construction of the murine adenosine deaminase (ADA) expression vector p9ADA5-29 has been described by Yeung *et al.* (1985). This plasmid contains the mouse DA cDNA sequence inserted into the *EcoRI* site of p91023(B) (Wong *et al.*, 1985). This plasmid encodes a dicistronic ADA and mouse DHFR transcript. A derivative of p9ADA5-29 lacking the adenovirus VA RNA genes was constructed by digestion of p9ADA5-29 and pL58 (Kaufman, 1985) with *BglII* (present in the intron for the transcription unit) and *SalI* (present in the tetracycline resistance gene), ligation of the large, ADA containing, fragment of p9ADA5-29 to the small, SV40 origin-containing fragment of pL58, and transformation of *Escherichia coli* to tetracycline resistance. The resultant plasmid p9A is identical to p9ADA5-29 except for the deletion of the adenovirus VA genes. The GM-CSF expression plasmid (pCSF-1) (Wong *et al.*, 1985) encodes a dicistronic CSF and DHFR transcript. In order to obtain a tricistronic expression plasmid, the CSF coding region (770 bp) was obtained from pCSF-1 by *EcoRI* digestion and inserted into the *EcoRI* site (5′ of the ADA sequence) in p9ADA5-29 to create p9CSF-ADA.

Cell culture

COS monkey cells were transfected using DEAE−dextran with the addition of a chloroquin treatment as described (Sompayrac and Dana, 1981; Luthman and Magnusson, 1983; Kaufman, 1985).

DHFR-deficient CHO cells (DUKX-B11) (Chasin and Urlaub, 1980) were transfected with the ADA−DHFR expression plasmid (p9ADA5-29) and selected initially for ADA expression and were then amplified in increasing concentrations of 2′-deoxycoformycin as described (Kaufman *et al.*, 1986a). Two clones 1−0.1 and 2−0.1 selected for resistance to 0.1 μM 2′-deoxycoformycin and the same clones selected for further resistance to 100 μM 2′-deoxycoformycin are designated 1−100 and 2−100, respectively, and have been described previously (Kaufman *et al.*, 1986a). Clone E6−0.1 is a DHFR-positive line selected to 0.1 μM MTX resistance after transfection of DHFR-deficient CHO cells with p91023(B).

pCSF-1 was introduced into DHFR-deficient CHO cells, DUKX-B11, by protoplast fusion as described by Sandri-Goldin *et al.* (1981). *E. coli* HB101 cells harboring pCSF-1 were grown in 50 ml of M9 salts containing 0.5% (w/v) casamino acids, 0.4% (w/v) glucose, 0.012% (w/v) $MgSO_4$, 5 μg/ml thiamine and 10 μg/ml tetracycline to an A_{600} of 0.6. Chloramphenicol was added to 250 μg/ml and the culture incubated at 37°C for an addition 16 h in order to amplify the plasmid copy number. A suspension of protoplasts was prepared as described by Sandri-Goldin *et al.* (1981), added to CHO DUKX-B11 cells at a ratio of ~1−2 $\times$ 10^8 protoplasts/cell, and centrifuged onto the cells at 2000 r.p.m. for 8 min in an IEC Model K centrifuge. After centrifugation, the supernatant was removed by aspiration and 2 ml of polyethylene glycol solution [150 g of PEG 1450 (Baker Chem. Co.) in 50 ml of medium] was added to each plate. Cells were centrifuged again at 2000 r.p.m. for 90 s, the PEG solution removed, and the plates rinsed three times in alpha medium containing 10% (v/v) fetal calf serum. Cells were then trypsinized and plated into tissue culture dishes in medium containing 100 μg/ml of kanamycin, 10 μg/ml each of thymidine, adenosine, deoxyadenozine, penicillin and streptomycin. Two days later the cells were trypsinized and subcultured 1:15 into media with 10% dialyzed fetal calf serum, penicillin and streptomycin, but lacking the nucleosides. Seven independent colonies that appeared after 12 days were trypsinized and combined into a single pool and grown in alpha medium lacking nucleosides (Kaufman *et al.*, 1985). These cells were subsequently grown in stepwise increasing concentrations of MTX starting at 0.02 μM, with sequential increases to 0.1, 0.5 and 2.0 μM, in order to obtain cells which had amplified the copy number of the GM-CSF gene. The selected population in 0.5 μM MTX was cloned by dilution plating in microtitre plates in alpha medium containing 10 μg/ml of penicillin, streptomycin and 10% (v/v) dialyzed fetal calf serum with 0.5 μM MTX. Clones obtained in 0.5 μM MTX were expanded and subsequently selected for growth in 2.0 μM MTX. Cells propagated in 0.02, 0.1, 0.5 and 2.0 μM MTX produced 2000, 4000, 12 000 and 50 000 units/ml/10^6 cells/day of GM-CSF, respectively, as determined by the colony formation assay with the KG-1 human myeloid leukemia cell line as described (Wong *et al.*, 1985).

Protoplast fusion yielded greater transfection efficiencies than $CaPO_4$-mediated DNA transfection and were necessary in order to obtain the rare transformants that efficiently express the polycistronic transcript. The inability to select for DHFR expression from polycistronic vectors in previous experiments (Kaufman *et al.*, 1985) was due to inefficient methods of DNA transfer.

Analysis of GM-CSF, ADA and DHFR expression

GM-CSF, ADA and DHFR synthesis were monitored by labeling of either transfected COS cells or CHO cells for 1 h with 100 μCi of L-[^{35}S]methionine (sp. act. >8000 Ci/mmol, New England Nuclear). Cell extracts were prepared and analysed by SDS−polyacrylamide gel electrophoresis, either before or after immunoprecipitation with a rabbit anti-human GM-CSF antibody (kindly provided by E.Wang, Genetics Institute), a sheep anti-mouse ADA antibody (Ingolia *et al.*, 1985), or a rabbit anti-mouse DHFR antibody. *Staphylococcus aureus* was used as the immunoadsorbant as described (Kaufman and Sharp, 1982a). The ADA and DHFR antisera were kindly provided by Rodney Kellems, Baylor University. Gels were fixed in 30% methanol, 10% acetic acid and 10% trichloroacetic acid,

and prepared for fluorography by treatment with EnHance (New England Nuclear Corp.), and dried. Dried gels were autoradiographed with Kodak XAR-5 film on a Du Pont Cronex Lightning-Plus screen. Protein levels were quantitated by visual comparison of band intensities from multiple autoradiograms of different exposure times.

Total RNA was prepared by guanidine thiocyanate extraction (Chirgwin *et al.*, 1979) and was examined by blot hybridization (Thomas, 1980) following electrophoresis on formaldehyde–formamide denaturing agarose gels and transfer to nitrocellulose as described by Derman *et al.* (1981). Hybridization was carried out using gel-isolated restriction fragments which had been labeled with [α-^{32}P]dATP by nick translation (Rigby *et al.*, 1977). The DHFR probe was derived from a *Pst*I digestion of pDHFR26 (Chang *et al.*, 1978) and the GM-CSF probe was derived from an *Eco*RI digestion of pCSF-1 (Wong *et al.*, 1985). Both these probes contain the intact coding region for the respective polypeptides.

Acknowledgements

We gratefully thank Louise Fouts for development and characterization of the GM-CSF producing cell line and Andrew Dorner and Clive Wood for critical reading of the manuscript.

References

Box,J.L., Polder,L.J., Bernards,R., Schrier,P.I., van den Elsen,P.J., van der Eb,A.J. and van Ormondt,H. (1981) *Cell*, **27**, 121–131.

Chang,A.C.Y., Nunberg,J.H., Kaufman,R.J., Erlich,H.A., Schimke,R.T. and Cohen,S.N. (1978) *Nature*, **275**, 617–624.

Chasin,L.A. and Urlaub,G. (1980) *Proc. Natl. Acad. Sci. USA*, **78**, 5334–5338.

Chirgwin,J.M., Przybyla,A.E., MacDonald,R.J. and Rutter,W.J. (1979) *Biochemistry*, **18**, 5294–5299.

Clerx-van Haaster,C., Akatshi,H., Auperin,C. and Bishop,D. (1982) *J. Virol.*, **41**, 119–128.

Derman,E., Krauter,K., Walling,L., Weinbergern,C., Ray,M. and Darnell,J.E. Jr. (1981) *Cell*, **23**, 731–739.

Dixon,L. and Hohn,T. (1984) *EMBO J.*, **3**, 2731–2736.

Ghosh,P.K., Reddy,V.B., Swinscoe,J., Lebowitz,P. and Weissman,S.M. (1978) *J. Biol. Chem.*, **253**, 3643–3647.

Hagenbuchle,O., Tosi,M., Schibler,U., Bovey,R., Wellauer,P.K. and Young, R.A. (1981) *Nature*, **289**, 643–646.

Haynes,J. and Weissman,C. (1983) *Nucleic Acids Res.*, **11**, 687–706.

Hendy,G., Kronenberg,H., Potts,J., Jr. and Rich,A. (1981) *Proc. Natl. Acad. Sci. USA*, **78**, 7365–7369.

Herman,R.C. (1986) *J. Virol.*, **58**, 797–804.

Hughes,S., Mellstrom,K., Koslik,E., Tamanoi,R. and Brugge,J. (1984) *Mol. Cell. Biol.*, **4**, 1738–1746.

Ingolia,D.E., Yeung,C.-Y., Grengo,J.F., Harrison,M.L., Frayne,E.G., Rudolph, F.B. and Kellems,R.E. (1985) *J. Biol. Chem.*, **260**, 13261–13267.

Kaufman,R.J. (1985) *Proc. Natl Acad. Sci. USA*, **82**, 689–693.

Kaufman,R.J. and Sharp,P.A. (1982a) *J. Mol. Biol.*, **159**, 601–621.

Kaufman,R.J. and Sharp,P.A. (1982b) *Mol. Cell. Biol.*, **2**, 1304–1319.

Kaufman,R.J., Sharp,P.A. and Latt,S.A. (1983) *Mol. Cell. Biol.*, **3**, 699–711.

Kaufman,R.J., Wasley,L.C., Spiliotes,A.J., Gossels,S.D., Latt,S.A., Larsen,G.R. and Kay,R.M. (1985) *Mol. Cell. Biol.*, **5**, 1750–1759.

Kaufman,R.J., Murtha,P., Ingolia,D.E., Yeung,C.-Y. and Kellems,R.E. (1986a) *Proc. Natl. Acad. Sci. USA*, **83**, 3136–3140.

Kaufman,R.J., Wasley,L.C., Furie,B.C., Furie,B. and Shoemaker,C.B. (1986b) *J. Biol. Chem.*, **261**, 9622–9268.

Kitajewshi,J.K., Schneider,R.J., Safer,B., Munemitsu,S.M., Samuel,C.E., Thimmappaya,B. and Shenk,T. (1986) *Cell*, **45**, 195–200.

Kitamura,N., Semler,B.L., Rothberg,P.G., Larsen,G.R., Adler,C.J., Dorner, A.J., Emini,E.A., Hanecak,R., Lee,J.J., van der Werf,S., Anderson,C.W. and Wimmer,E. (1981) *Nature*, **291**, 547–553.

Konarska,M., Filipowicz,W., Domday,H. and Gross,H.J. (1981) *Eur. J. Biochem.*, **114**, 221–227.

Kozak,M. (1979a) *Nature*, **280**, 82–85.

Kozak,M. (1979b) *J. Biol. Chem.*, **254**, 4731–4738.

Kozak,M. (1980a) *Cell*, **22**, 7–8.

Kozak,M. (1980b) *Cell*, **22**, 459–468.

Kozak,M. (1984) *Nucleic Acids Res.*, **12**, 3873–3893.

Kozak,M. (1986) *Proc. Natl. Acad. Sci. USA*, **83**, 2850–2854.

Kozak,M. and Shatkin,A.J. (1978) *J. Biol. Chem.*, **253**, 6568–6577.

Lau,Y.-F., Lin,C.C. and Kan,Y.W. (1984) *Mol. Cell. Biol.*, **4**, 1469–1475.

Liu,C.C., Simonsen,C.C. and Levinson,A.D. (1984) *Nature*, **309**, 82–85.

Luthman,H. and Magnusson,G. (1983) *Nucleic Acids Res.*, **11**, 1295–1308.

Marsden,H.S., Haarr,L. and Preston,C.M. (1983) *J. Virol.*, **46**, 434–445.

McCormick,F., Trabey,M., Innis,M., Dieckmann,B. and Ringold,G. (1984) *Mol. Cell. Biol.*, **4**, 166–172.

Mellon,P., Parker,V., Gluzman,Y. and Maniatis,T. (1981) *Cell*, **27**, 279–288.

Mertz,J.E., Murphy,A. and Barkan,A. (1983) *J. Virol.*, **45**, 36–46.

O'Malley,R.P., Mariano,T.M., Siekierka,J. and Mathews,M.B. (1986) *Cell*, **44**, 391–400.

Peabody,D.S. and Berg,P. (1986) *Mol. Cell. Biol.*, **6**, 2695–2703.

Peabody,D.S., Subramani,S. and Berg,P. (1986) *Mol. Cell. Biol.*, **6**, 2704–2711.

Pelletier,J. and Sonenberg,N. (1985) *Cell*, **40**, 515–526.

Perler,H., Efstratiadis,A., Lomedico,P., Gilbert,W., Kolodner,R. and Dogson,J. (1980) *Cell*, **20**, 555–566.

Reichel,P.A., Merrick,W.C., Siekierka,J. and Mathews,M.B. (1985) *Nature*, **313**, 196–200.

Rigby,P.W., Dieckmann,M., Rhodes,C. and Berg,P. (1977) *J. Mol. Biol.*, **113**, 237–251.

Sandri-Goldin,R.M., Goldin,A.L., Levine,M. and Glorioso,J.C. (1981) *Mol. Cell. Biol.*, **1**, 743–752.

Scahill,S.J., Devos,R., Heyden,J.V. and Fiers,W. (1983) *Proc. Natl. Acad. Sci. USA*, **80**, 4654–4658.

Shatkin,A.J. (1976) *Cell*, **9**, 645–653.

Sompayrac,L.M. and Dana,K.J. (1981) *Proc. Natl. Acad. Sci. USA*, **78**, 7575–7578.

Svensson,C. and Akusjarvi,G. (1984) *Mol. Cell. Biol.*, **4**, 736–742.

Svensson,C. and Akusjarvi,G. (1985) *EMBO J.*, **4**, 957–964.

Swanstrom,R., Varmus,H.E. and Bishop,J.M. (1982) *J. Virol.*, **41**, 535–541.

Thomas,P.S. (1980) *Proc. Natl. Acad. Sci. USA*, **77**, 5201–5205.

Vogeli,G., Ohkubo,H., Sobel,M.E., Yamada,Y., Pastan,I. and de Crombrugghe, B. (1981) *Proc. Natl. Acad. Sci. USA*, **78**, 5334–5338.

Wengler,G., Wengler,G. and Gross,H.J. (1979) *Nature*, **282**, 754–756.

Yeung,C.-Y., Ignolia,D.E., Roth,D.B., Shoemaker,C., Al-Ubaidi,M.R., Yen, J.-Y., Ching,C., Bobonis,C., Kaufman,R.J. and Kellems,R.E. (1985) *J. Biol. Chem.*, **260**, 10299–10307.

Yoo,O.J., Powell,C.T. and Agarwal,K.L. (1982) *Proc. Natl. Acad. Sci. USA*, **79**, 1049–1053.

Wong,G.G., Witek,J.S., Temple,P.A., Wilkens,K.M., Leary,A.C., Luxenberg, D.P., Jones,S.S., Brown,E.L., Kay,R.M., Orr,E.C., Shoemaker,C.S., Golde, D.W., Kaufman,R.J., Hewick,R.M., Wang,E.A. and Clark,S.C. (1985) *Science*, **228**, 810–815.

Received on 3 November 1986

EXHIBIT B

MOLECULAR AND CELLULAR BIOLOGY, Dec. 1991, p. 5848–5859
0270-7306/91/125848-12$02.00/0

Vol. 11, No. 12

The Encephalomyocarditis Virus Internal Ribosome Entry Site Allows Efficient Coexpression of Two Genes from a Recombinant Provirus in Cultured Cells and in Embryos

INGRID R. GHATTAS,[1] JOSHUA R. SANES,[2] AND JOHN E. MAJORS[1]*

Departments of Biochemistry and Molecular Biophysics[1] and of Anatomy and Neurobiology,[2] Washington University School of Medicine, 660 South Euclid Avenue, St. Louis, Missouri 63110

Received 16 June 1991/Accepted 3 September 1991

Rous sarcoma virus-based retroviral vectors were constructed to compare three different approaches for coexpressing two genes in individual infected cells. All vectors expressed the upstream gene (*lacZ*) from the Rous sarcoma virus long terminal repeat, while the downstream gene (the chloramphenicol acetyltransferase gene [*cat*] or v-*src*) was expressed in one of three ways: from a subgenomic mRNA generated by regulated splicing, from a strong internal promoter, or from the encephalomyocarditis virus internal ribosome entry site (IRES). Both biochemical and immunohistochemical assays of cultured cells showed that the encephalomyocarditis virus IRES provided the most efficient means for coexpressing two genes from a single provirus. Most importantly, most cells infected by a LacZ–IRES-CAT virus expressed both LacZ and CAT, whereas most cells infected by internal promoter or regulated splicing vectors expressed either LacZ or CAT but not both. In addition, viral titers were highest with IRES vectors. Presumably, use of the IRES avoids transcriptional controls and RNA processing steps that differentially affect expression of multiple genes from internal promoter and regulated splicing vectors. Finally, we injected a LacZ–IRES–v-Src virus into chicken emhryos and then identified the progeny of infected cells with a histochemical stain for LacZ. LacZ-positive cells in both skin and mesenchyme displayed morphological ahnormalities attributable to expression of v-*src*. Taus, IRES vectors can be used to coexpress a reporter gene and a bioactive gene in vivo.

When a retrovirus infects a cell, the viral genome is stably integrated into the host chromosome, efficiently expressed, and faithfully passed to the infected cell's progeny. For these reasons, recombinant retroviral vectors have often been used to express exogenous genes in vertebrate cells (reviewed in references 28, 34, and 52). In some of these cases, it is advantageous to express two exogenous genes from a single proviral genome. In strategies being developed for gene therapy, for example, the retrovirus often contains not only the gene of interest but also a selectable marker. The marker is used to facilitate the isolation of infected cells, which are then used as a source of the potentially therapeutic gene product (reviewed in reference 12).

In another set of studies, we and others have used vectors encoding the histochemical marker β-galactosidase, the product of the *Escherichia coli lacZ* gene, as lineage tracers in vivo. A single cell is infected by a retrovirus, the proviral genome is inherited by the cell's progeny, and the clonal relatives are identified with the histochemical stain for LacZ (11, 13, 16, 18, 45; reviewed in reference 17). To extend this work, we wished to construct an efficient double-expression vector to transfer both *lacZ* and a second gene to single cells in vivo. If *lacZ* and a second bioactive gene were reliably coexpressed at high levels, we could use LacZ histochemistry to identify small clones of transgenic cells in a wild-type environment and then seek cell autonomous effects of the second gene by analyzing the number, distribution, and morphology of the labeled cells.

In applications such as these, it is essential that the provirus express both genes within the same individual cells. Retroviruses have been successful in evolving strategies for coexpressing their own genes. These strategies include synthesis and subsequent processing of fusion proteins, ribosome frameshifting, and regulated splicing to generate subgenomic messages. Unfortunately, achieving balanced expression of multiple exogenous genes from engineered retrovirus vectors has been more problematic. Two approaches have been used previously. The first involves the generation of separate mRNAs by regulated splicing of a single primary transcript expressed from the upstream long terminal repeat (LTR). This strategy mimics that used by retroviruses to generate the *env* gene product (54). With this approach, expression of one gene is always at the expense of the other, and the ratio of spliced to unspliced mRNA is highly dependent on the context (1, 2, 48, 49). The second approach involves expression of the upstream gene from the retrovirus promoter in the LTR and expression of the downstream gene from an internal promoter. This approach has been used most often in vectors designed for gene therapy (reviewed in references 28 and 34) but is compromised by competitive interference between promoters (4, 8, 20, 39). Thus, individual isolates may express one gene or the other, rather than both.

The recent demonstration that the 5′ nontranslated region of encephalomyocarditis virus (EMCV) and other picornaviruses allows translation initiation from the internal ribosome entry site (IRES) (22–24) has suggested a third strategy for expressing multiple genes from a single proviral genome: the viral LTR can be used to express a single polycistronic transcript from which several gene products are translated. In this way, transcriptional controls and RNA processing steps that differentially affect expression of multiple genes can be avoided. In this study, we have used three pairs of genes to compare this approach with the double-promoter and regulated-splicing strategies. Biochemical and immuno-

* Corresponding author.

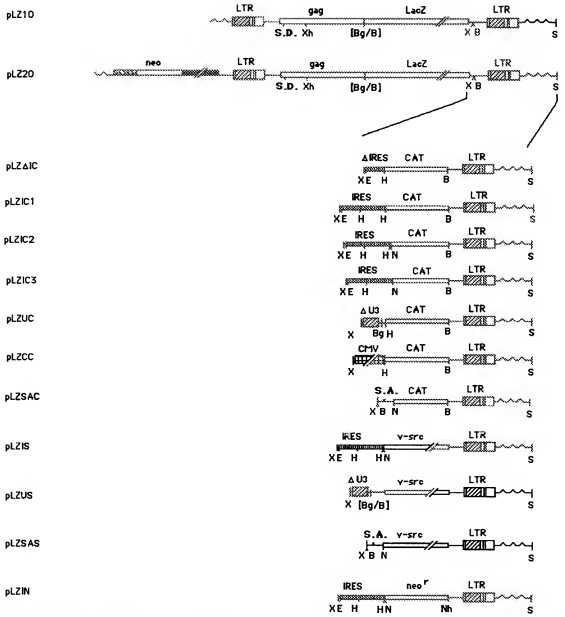

FIG. 1. Structures of retrovirus vectors used in this study. Notation: straight lines, RSV sequences; wavy lines, bacterial sequences; diagonal lines, truncated U3 region of RSV; squares, CMV immediate-early promoter; vertical lines, sequences of the EMCV 5' nontranslated region; spotted and dark stippled boxes, SV40 promoter and SV40 poly(A) signal, respectively; S.A., splice acceptor site; S.D., splice donor site; B, *Bam*HI; Bg, *Bgl*II; E, *Eco*RI; H, *Hin*dIII; N, *Nco*I; Nh, *Nhe*I; S, *Sal*I; X, *Xba*I; Xh, *Xho*I. Brackets indicate sites destroyed by ligation. The diagrams are roughly to scale.

histochemical assays indicate that the EMCV IRES is more effective than either the double-promoter or the regulated-splicing strategy at expressing two exogenous genes from a single proviral genome. Using an EMCV IRES vector that encodes LacZ and v-Src, we then infected chicken embryos in ovo. We show that LacZ-positive cells in the skin and meninges consistently express morphological abnormalities that are attributable to v-*src*.

MATERIALS AND METHODS

Plasmid constructions. DNA manipulations were done by standard methods (44). The main features of the plasmids described below are illustrated in Fig. 1.

All vector plasmids are derivatives of pLZ20, which is similar to the previously described pLZ10 (13) except for the addition within the plasmid of a Tn5 neomycin resistance gene (*neo*) flanked by a simian virus 40 (SV40) promoter and

poly(A) signal. Both pLZ10 and pLZ20 are derived from the SRA-2 molecular clone of the Rous sarcoma virus (RSV) genome (50) and produce LacZ as a freely soluble Gag-LacZ fusion protein. For each new vector, the *Xba*I-*Sal*I fragment of pLZ20 was replaced by a different fragment of interest. Plasmid pLZAIC contains a truncated EMCV IRES extending from the *Eco*RI site at nucleotide (nt) 2334 to the *Hin*dIII site at nt 2566 of pE5LVP0 (40); nt 2334 of the plasmid is equivalent to nt 260 of the EMCV 5′ nontranslated region. This fragment was linked to a 773-bp *Hin*dIII-*Bam*HI fragment of pSV2CAT which contains the bacterial chloramphenicol acetyltransferase (*cat*) gene (15). The IRES fragment in pLZIC1 extends from nt 2334 to the EMCV initiation codon at nt 2915, which was converted to a *Hin*dIII site (conversion from AAUAUGGCC to AAGCUUGCC extending from nt 2912 to 2920 of pE5LVP0) by site-directed mutagenesis (36). The oligonucleotide ACACGAATGATA AGCTTGCCACAACCA used for mutagenesis was obtained from the protein chemistry laboratory at Washington University. In pLZIC2, pLZIC3, pLZIS, and pLZIN, the EMCV sequence extends to an *Nco*I site 9 bp downstream of the EMCV initiation codon, which was altered in the cases of pLZIC2, pLZIS, and pLZIN. The *cat* gene in pLZIC2 and pLZIC3 has a 29-bp sequence of the 5′ nontranslated *cat* region deleted and the initiation codon converted to an *Nco*I site. The *Xba*I-*Bgl*II fragment in pLZUC and pLZUS includes a truncated RSV U3 region, extending from nt -220 (an artificial *Bam*HI site) to -10 (a *Taq*I site), joined to a short linker sequence ATACCGTCCCAGATCT. To generate pLZUC, this fragment was linked to the *Hin*dIII end of the *cat* fragment by using a 56-bp *Sfi*I-*Hin*dIII filler fragment derived from the SV40 T-antigen leader sequence that was modified at the *Sfi*I end by addition of a *Bgl*II linker. pLZCC was derived from pLZIC1 by substitution of the *Xba*I-*Hin*dIII EMCV fragment with a 780-bp *Xba*I-*Hin*dIII fragment that harbors the enhancer/promoter region of a cytomegalovirus (CMV) immediate-early gene (3). The v-*src* splice acceptor site used in pLZSAC is derived from the region upstream of SRA v-*src* and was transferred as a *Bam*HI-*Nco*I fragment from a previously described construction (21). The v-*src* gene in pLZIS, pLZUS, and pLZSAS was derived from this same construction and was transferred as a *Bam*HI-*Eco*RI fragment into pLZUC and pLZSAC to make pLZUS and pLZSAS and as an *Nco*I-*Eco*RI fragment to make pLZIS. Finally, the *Nco*I-*Nhe*I fragment of pLZIN, which includes the *neo* gene, was generated by the polymerase chain reaction, using primers which converted the *neo* AUG to an *Nco*I site and introduced an *Nhe*I site immediately downstream of the translation termination site. Joining to the 3′ LTR was effected by introduction of an *Nhe*I linker at the *Bam*HI site that separates the CAT sequences in pLZIC1 from the downstream viral sequences. The helper plasmid employed in these experiments used the CMV promoter fragment described above to promote expression of SRA viral sequences that extended from a *Sac*I site 120 bp 5′ to the *gag* AUG (6) to an *Rsa*I site 6 bp 3′ to the end of *env* (5). A polyadenylation signal was provided from the herpes simplex virus *tk* gene (32).

Transfections and virus recovery. These experiments used QT6 cells, a chemically transformed quail fibroblast cell line (37). Cells were grown at 37°C and 5% CO_2 in Earle's 199 medium supplemented with 5% tryptose phosphate buffer, 5% fetal bovine serum, 1% dimethyl sulfoxide, penicillin, and streptomycin. Cells were plated at 2×10^6 cells per 60-mm dish 24 h prior to transfection and were fed fresh medium 1 h before transfection. The cells were transfected by the calcium phosphate procedure (53) with one of the recombinant plasmids and the helper plasmid, which provided the viral genes necessary to produce viral particles. The calcium phosphate coprecipitates were formed by using 6 μg each of the recombinant and helper plasmids. Seven hours after the precipitate had been added, the cells were treated with dimethyl sulfoxide as described by Lopata et al. (31). The cells were then incubated for 40 h before the virus-containing media were harvested and cell extracts were made.

The harvested media were passed through a 0.45-μm-pore-size filter to remove intact cells, and Polybrene was added to a final concentration of 8 μg/ml to enhance the efficiency of infection. The virus-containing media were then added to fresh QT6 cells, which were grown for at least 48 h before expression of virus-encoded genes was assessed as described below.

Enzyme assays. Extracts of transfected cells were prepared by three cycles of freezing and thawing in 100 μl of 0.25 M Tris-HCl (pH 8.0), followed by centrifugation at 4°C for 5 min to remove cell debris. LacZ activity was measured by the method of Miller (35), with the amounts of extract and time of incubation adjusted so that the A_{420} was between 0.2 and 1. CAT activity was measured by the method of Gorman et al. (15). Briefly, extract of transfected cells was added to a reaction mixture containing 37.5 μl of Tris-HCl (pH 7.5), 1 μl of 50-mg/ml chloramphenicol, and 0.1 μCi of [^{14}C]chloramphenicol (60 mCi/mmol; New England Nuclear Corp.). The mixture was adjusted to a final volume of 135 μl and preincubated for 5 min at 37°C. The reaction was then started by adding 15 μl of 50 mM acetyl coenzyme A. The amount of extract was adjusted so that the percent conversion of the nonacetylated form to the acetylated form of chloramphenicol was between 10 and 50%. For CAT assays on infected cells, unlabeled chloramphenicol was omitted.

Histochemistry. For histochemical staining of cells expressing the LacZ gene product, cells were fixed in 2% formaldehyde in phosphate-buffered saline (PBS) for 10 min. The cells were then stained for LacZ at room temperature, overnight, in a mixture containing 1 mg of 5-bromo-4-chloro-3-indolyl-β-D-galactoside (X-Gal) per ml, 4 mM potassium ferricyanide, 4 mM potassium ferrocyanide, and 2 mM $MgCl_2$ in PBS (45). For immunohistochemical detection of LacZ and CAT, infected cells were seeded on coverslips 24 h prior to staining. The cells were fixed in 1% formaldehyde in PBS for 30 min and then incubated with antibodies. Primary antibodies were mouse monoclonal anti-β-galactosidase, prepared in our laboratories, rabbit anti-CAT (5 Prime → 3 Prime Inc., West Chester, Pa.), and rabbit antiserum to bacterially produced v-Src, generously provided by P. Maness, University of North Carolina (33). Secondary antibodies were (i) fluorescein-conjugated goat anti-mouse immunoglobulin G (IgG) plus IgM and (ii) rhodamine-conjugated goat anti-rabbit IgG (Boehringer Mannheim, Indianapolis, Ind.). For LacZ and CAT, each incubation was for 30 min at room temperature in PBS containing 5% goat serum and 0.01% Triton X-100. The v-*src* gene product was detected by incubating the cells overnight at 4°C with primary antibody, followed by a 30-min incubation with biotin-conjugated anti-rabbit IgG (Sigma, St. Louis, Mo.) and a 30-min incubation with Texas red-conjugated streptavidin (Bethesda Research Laboratories). Finally, coverslips were washed with PBS and mounted in 80% glycerol-*p*-phenylenediamine.

Infection of embryos. Methods for inoculation of embryos

and processing of tissue have been described previously (13, 16, 29). Briefly, fertilized White Leghorn eggs were obtained from SPAFAS (Roanoke, Ill.) and incubated at 37°C. Embryos were exposed through a window in the shell and staged by the criteria of Hamburger and Hamilton (19). Virus was concentrated from the medium of virus-producing QT6 cells by centrifugation, mixed with fast green and Polybrene, and drawn into a 10- to 30-μm-tip glass capillary microelectrode. A total of 0.5 to 3 μl of this mixture was pressure injected over the skin, subdermally, and into the lumen of the neural tube. No attempt was made to limit the injections to particular regions of the embryo. The shell was then closed with tape, and the egg was returned to the incubator.

At appropriate times thereafter, embryos were recovered, eviscerated, fixed for 1 h with 2% formaldehyde plus 0.4% gluteraldehyde in PBS, washed thoroughly in PBS, incubated overnight in X-Gal solution (see above), rinsed in PBS, and refixed in 2% formaldehyde–2% gluteraldehyde. The embryos were then examined under a dissecting microscope at ×20 to ×40. Small pieces of tissue bearing LacZ-positive cells were cut out and either mounted whole in 90% glycerol–10% PBS or dehydrated in ethanol, embedded in Araldite, and sectioned at 5 μm.

RESULTS

In this study, we compared three different strategies for coexpressing *lacZ* and a downstream gene from RSV-based retrovirus vectors. The upstream gene was always fused in frame with the *gag* polyprotein and expressed from the LTR of the SRA-2 clone of RSV (50). The downstream gene was expressed in one of three ways: from a spliced subgenomic message, from an internal promoter, or from the EMCV IRES. To generate spliced mRNA from primary transcripts, we used the splice acceptor site of the RSV v-*src* gene (51). In these vectors, the RSV LTR promotes expression of primary transcripts, which are either used intact for packaging and for translation of the upstream gene or spliced to form a subgenomic RNA from which the downstream gene is translated. In cells infected with the wild-type RSV, about half of the primary transcripts are spliced to generate *env* and v-*src* subgenomic mRNAs, although the precise ratio of spliced to unspliced RNA varies among strains (49). For an internal promoter, we used a fragment of the U3 region of the RSV LTR (50). This fragment includes promoter and enhancer sequences but excludes both the inverted repeat sequence at the 5′ end, which is required for integration, and the polyadenylation signal at the 3′ end. In one vector, we also used the immediate-early promoter of CMV as an internal promoter. Finally, a fragment of EMCV that contains an IRES was used to promote internal ribosome binding. *lacZ* was paired with three genes for these tests: *cat*, because a simple and sensitive test is available for its products; v-*src*, because we expected it to alter cellular morphology in ways that would be detectable in vivo; and *neo*, because it is a selectable marker that can be used in studies of transcriptional activation.

Structure of the EMCV IRES fragment. Translation of EMCV mRNA occurs in a cap-independent fashion: ribosomes bind internally at the initiating AUG without scanning the 5′ nontranslated region of the transcript. Sequences between nt 403 and 811 of the EMCV 5′ nontranslated region are required for efficient translation. They include a stem-loop structure which interacts with a 57-kDa cellular protein and a stretch of pyrimidine-rich sequences near the initiation codon, both of which are essential for IRES function (24). Synthesis of the EMCV polyprotein initiates at the 11th AUG codon, which is located in a perfect Kozak consensus sequence (27).

In earlier studies which used the IRES, the *cat* gene was expressed either from the EMCV initiation codon as a fusion protein (22) or from an engineered *Nco*I site placed at the EMCV initiation codon (7). We wanted to construct a vector in which foreign genes could be expressed either from their own initiation codons or from one in the vector. To do so, we took note that the 12th EMCV AUG, located 9 bp downstream of the EMCV initiation codon (the 11th AUG), is part of an *Nco*I site and is surrounded by a Kozak consensus sequence. To assess whether we could use that site as an initiation codon and to provide a site for insertion of genes with their own initiation codons, we converted the natural translation start site of the EMCV to a *Hind*III site. Thus, the sequence 5′-AAU **AUG** GCC ACA ACC **AUG** GAA-3′ was mutated to 5′-AAG CUU GCC ACA ACC **AUG** GAA-3′. The efficiency of translation from the 12th AUG was tested by placing the *lacZ* gene at that site in the wild-type context and in the altered context and then measuring the levels of LacZ in cells transfected with the two plasmids. Translation is presumed to start at the 11th AUG in the wild-type context but must start at the 12th AUG in the altered vector. Nonetheless, levels of LacZ were roughly the same in both cases (data not shown).

LacZ-CAT vectors. Unselected coexpression of the bacterial *lacZ* and *cat* genes was tested by expressing the upstream *lacZ* gene from the RSV LTR as a Gag-LacZ fusion protein and expressing the downstream *cat* gene in each of several ways: from a spliced subgenomic message (pLZSAC), from an internal RSV promoter (pLZUC), from an internal CMV promoter (pLZCC), or from EMCV IRES fragments (Fig. 1). Because our primary aim was to test the efficacy of the EMCV IRES strategy, and because the distance between the pyrimidine stretch in the IRES and the initiation codon has been reported to be critical (24), we constructed four different IRES-containing vectors (pLZIC1, pLZIC2, pLZIC3, and pLZΔIC). In the case of pLZIC1, the *cat* gene from pSV2CAT (15) was inserted at the new *Hind*III site of the EMCV IRES fragment (see above). In this vector, a 29-bp sequence of the CAT 5′ nontranslated region separates the CAT initiation codon from the 3′ end of the EMCV IRES. To assess the effect of this separation on CAT expression, we also converted the CAT initiation codon to an *Nco*I site and joined it to the *Nco*I site of either the altered EMCV IRES (pLZIC2) or the wild-type EMCV IRES (pLZIC3). Finally, plasmid pLZΔIC was constructed as a control for internal initiation, with the *cat* gene placed at the upstream *Hind*III site of the EMCV fragment. The EMCV fragment was only 232 bp long in this case and did not include the entire IRES sequence.

QT6 cells were transfected with each plasmid to confirm the integrity of the two genes. Cell extracts were prepared 40 h after transfection, and CAT activity relative to LacZ activity was measured (Table 1). All of the vectors expressed LacZ, and all except pLZΔIC expressed CAT, but the ratios of CAT to LacZ varied among them. The relative levels of CAT expression were roughly twofold higher when the *cat* gene was placed directly at the 3′ end of the EMCV IRES (pLZIC2 and -3) than when it was separated by a 29-bp untranslated fragment (pLZIC1) or expressed from the RSV promoter (pLZUC). The highest levels of CAT expression were obtained from the CMV promoter, which was previously shown to be more powerful than the RSV promoter in mammalian expression vectors (10). CAT expression from a

TABLE 1. Gene expression LacZ-CAT vectors

Vector	Relative CAT activity (%)[a]	
	In transfected cells	In infected cells
pLZAIC	0.6	0.75
pLZIC1	49, 48	46, 62
pLZIC2	89, 84	75, 101
pLZUC	26, 58	68
pLZCC	274, 468	56, 74
pLZSAC	5, 6	4, 4

[a] For each vector, the amount of CAT activity was determined per unit of LacZ activity in the same extract. These values were then expressed as percentages of the values from pLZIC3-transfected or -infected cells. Numbers from two independent experiments are represented. CAT activities in pLZAIC-infected or -transfected cells were similar to those of mock-transfected or -infected cells.

spliced message was only 5 to 10% that of the IRES vectors. There was no CAT expression from the 232-bp EMCV fragment of pLZΔIC, which confirms the requirement of an IRES for internal initiation. Thus, the ratio of CAT to LacZ activities depended on the mechanism used to drive expression of CAT.

To test for virus particle production and for expression of the *lacZ* and *cat* genes from a proviral genome, virus particles were generated by cotransfection of QT6 cells with a helper plasmid and one of the retroviral plasmids. Media were collected 40 h after transfection and used to infect fresh QT6 cells. After another 48 h, the infected cells were assayed in three ways. First, we estimated the number of LacZ infectious units per microgram of transfected DNA (LacZ titers) by staining with X-Gal and counting the resulting blue cells. LacZ titers were consistently higher from the IRES vectors than from the other proviruses. For example, in five experiments in which pLZIC1 and the U3 internal promoter vector were directly compared, the titer of the double-promoter vector was 23% ± 4% (mean ± standard error of the mean) that of the IRES vector. Thus, even if LacZ titers underestimate true titers of the double-promoter vector by twofold (see below), the IRES vectors still produce higher levels of viral particles. Similarly, in a single experiment, the LacZ titers of pLZSAC and pLZCC were found to be 35 and 40% that of pLZIC1, respectively. These results are consistent with the possibilities that negative interactions between promoters partially inhibit the production of genomic RNA from the LTR (8, 9) and that expression of spliced subgenomic mRNA is at the expense of full-length genomic RNA (see below).

Second, we estimated the amount of CAT expression relative to LacZ expression by preparing cell extracts from the infected cells and assaying them for the two enzymes. As for the transfectants, more CAT than LacZ was expressed from vLZIC2 and vLZIC3 (v denotes the proviral state) than from vLXIC1, vLZUC, or vLZSAC (Table 1). Surprisingly, the ratio of CAT to LacZ was severalfold lower for vLZCC than for pLZCC. This difference may reflect an effect of the integrative state of the provirus, although this was not observed in mammalian cells (10). For the other six vectors, however, the relative expression of the two genes was not greatly affected by the state of integration.

The biochemical assays of infected cells showed that the levels of CAT relative to LacZ from the double-promoter and IRES vectors varied less than twofold. They did not, however, address the issue of whether both genes are reliably coexpressed within individual cells. To test for coexpression, we performed a third set of assays in which we doubly stained infected cultures with antibodies to LacZ and CAT. Cells from infected cultures were seeded on coverslips 40 h after infection and grown for another 24 h. The cells were then fixed and stained with rhodamine-tagged anti-CAT and fluorescein-tagged anti-LacZ. As shown in Fig. 2 and Table 2, the extent of coexpression varied greatly among vectors. More than 90% of the vLZIC1-, -2-, and -3-infected cells that were LacZ positive were also CAT positive. In contrast, in vLZUC-infected cultures, only 6% of infected cells were stained for both CAT and LacZ; two-thirds of the infected cells made detectable levels of only the upstream *lacZ* gene, and one-quarter expressed only the downstream *cat* gene. This result suggests that the two promoters in the vector interfered with each other. To determine whether the interfering effect of the two promoters occurred only when the two promoters in the vector were identical, we substituted the internal U3 fragment with a fragment harboring an immediate-early CMV promoter. In this case, expression of LacZ and CAT was also noncoordinate in most (60%) of the infected cells; the other 40% stained positively for both LacZ and CAT. There was little CAT staining detectable above background in the vLZSAC-infected cells and none in the vLZΔIC-infected cells. The low levels of CAT activity measured by enzymatic assays in cells infected with vLZSAC presumably limited detection by immunostaining. Thus, IRES vectors direct more reliable coexpression of LacZ and CAT than do double-promoter or regulated-splicing vectors.

LacZ–v-Src vectors. To test the general utility of the IRES approach for expressing two genes from a proviral genome, we constructed a second set of vectors in which the viral oncogene v-*src* was placed downstream of the *lacZ* gene (Fig. 1). The downstream v-*src* gene was expressed from a spliced subgenomic mRNA (pLZSAS), from an internal RSV promoter (pLZUS), or from the EMCV IRES fragment (pLZIS). In all vectors, LacZ was expressed as a Gag-LacZ fusion protein from the 5′ LTR, and gene expression was estimated by visual inspection of immunohistochemically stained infected cells.

Virus particles were generated by cotransfection of QT6 cells with a helper plasmid and a LacZ–v-Src vector. Media were harvested 40 h after transfection and used to infect fresh QT6 cells. The vector pLZ20, which expresses LacZ alone, was used as a control. The infected cells were stained with X-Gal 48 h after infection to estimate LacZ titers. LacZ titers from four independent experiments indicated that the LacZ titers of pLZUS and pLZSAS were 8% ± 3% and 16% ± 10% that of pLZIS. This order is the same as that observed with the LacZ-CAT vectors and supports the idea that production of subgenomic RNA occurs at the expense of genomic RNA. The titers of vLZIS were 78, 125, and 169% those of vLZ20 in three experiments, indicating that insertion of the IRES does not interfere with virus production.

Coexpression in cells infected by LacZ–v-Src vectors was assessed by immunofluorescence using fluorescein-tagged anti-LacZ and Texas red-tagged anti-v-Src. Background staining by anti-v-Src was relatively high in all cultures, possibly because of cross-reaction of the antibody with endogenous c-Src. Nonetheless, specific staining attributable to v-Src was detectable, and it was evident that proviruses expressing v-Src from the EMCV IRES showed higher rates of coexpression than did the other two LacZ–v-Src proviruses (Fig. 3). Coexpression of LacZ and v-Src was

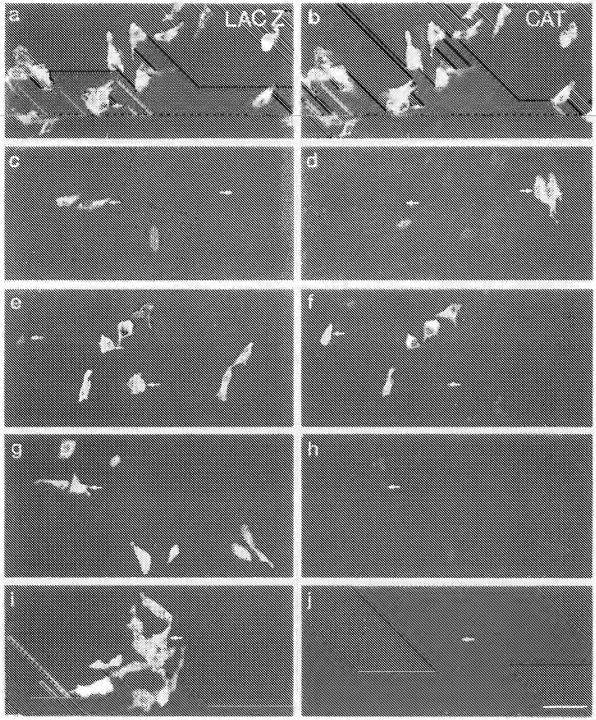

FIG. 2. Coexpression of LacZ and CAT from proviral genomes. Cultures of QT6 cells that had been infected with LacZ-CAT vectors were doubly stained with antibodies to LacZ and to CAT as described in Materials and Methods. Fields were then photographed with fluorescein optics to show LacZ (a, c, e, g, and i) and with rhodamine optics to show CAT (b, d, f, h, and j). Vectors were the IRES vector, pLZ/C1 (a and b); the internal U3 promoter vector, pLZUC (c and d); the internal CMV promoter, pLZCC (e and f); the regulated splicing vector, pLZSAC (g and h); and the truncated IRES vector, pLZΔIC (i and j). LacZ and CAT are reliably coexpressed only in pLZIC1-infected cells. Arrows mark corresponding points on the two micrographs of each pair. In all cultures, <5% of the cells were antibody stained; unstained cells are only barely visible in these micrographs. The bar represents 50 μm.

TABLE 2. Coexpression of LacZ and CAT in QT6 cells infected with LacZ-CAT vectors[a]

Vector	% of infected cells expressing:		
	CAT only	LacZ only	LacZ and CAT
pLZAIC	0	100	0
pLZIC1	3	0	97
pLZIC2	7	3	90
pLZIC3	2	2	96
pLZUC	25	69	6
pLZCC	34	26	40
pLZSAC	3	90	7

[a] Cells were doubly stained for CAT and LacZ as described in Materials and Methods. In each case, 200 stained cells were counted from randomly chosen fields.

detected in more than 90% of the vLZIS-infected cells but in less than 10% of the vLZUS- and vLZSAS-infected cells. Most of the vLZUS-infected cells that expressed LacZ stained weakly if at all above the background level with the v-Src antibody, and most of the v-Src-positive cells were negative for LacZ expression. In the case of vLZSAS-infected cells, there were roughly threefold more LacZ-positive than v-Src-positive cells, although again weak expression of v-Src might have been obscured by the endogenous immunoreactive material. Thus, LacZ and v-Src were more reliably coexpressed from the IRES vector than from the double-promoter or regulated-splicing vectors.

In examining the immunostained cultures, a second indication of v-Src expression became apparent: most v-Src-positive cells were rounded and refractile, as has been noted previously with fibroblasts infected or transfected with v-Src expression vectors (30). In vLZIS-infected cultures, most of the LacZ-positive cells detected immunohistochemically dis-

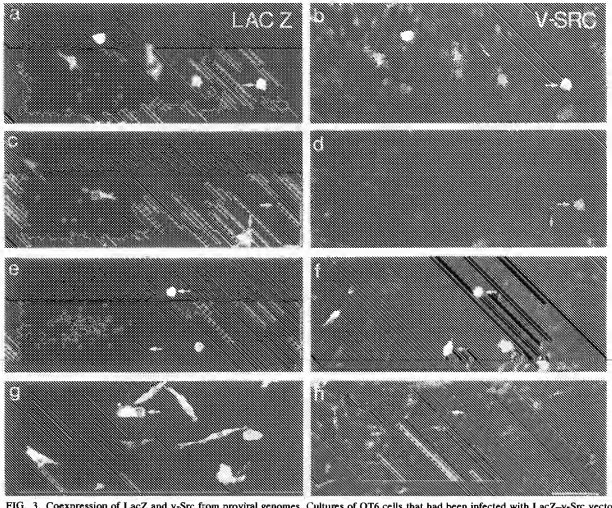

FIG. 3. Coexpression of LacZ and v-Src from proviral genomes. Cultures of QT6 cells that had been infected with LacZ–v-Src vectors were doubly stained with antibodies to LacZ and to v-Src as described in Materials and Methods. Fields were then photographed with fluorescein optics to show LacZ (a, c, e, and g) and with rhodamine to show v-Src (b, d, f, and h). Vectors were the IRES vector, pLZIS (a and b); the internal U3 promoter vector, pLZUS (c and d); the regulated-splicing vector, pLZSAS (e and f); and the LacZ-only vector, pLZ20 (g and h). LacZ and v-Src are reliably coexpressed only from pLZIS-infected cells. Arrows mark corresponding points on the two micrographs of each pair. The bar represents 50 μm.

played this altered phenotype, whereas most LacZ-positive cells were morphologically normal in vLZUS- and vLZSAS-infected cultures. This result supports the conclusion that vLZIS is the best of the three vectors tested at coexpressing LacZ and v-Src.

LacZ-Neo^r vector. As a third test of the IRES strategy, we constructed two vectors in which the *lacZ* and *neo* genes were separated by the EMCV IRES. In the first, the *lacZ* gene was expressed from the 5′ LTR as a Gag-LacZ fusion protein and the *neo* gene was placed downstream of the IRES sequence at the *Nco*I site (Fig. 1). In the second, the *neo* gene was expressed from the LTR as a Gag-Neo^r fusion protein and the *lacZ* gene was placed downstream of the IRES at the *Nco*I site. Virus was produced from both vectors and used to infect QT6 cells. Neo^r cells were selected by growth in G418 and stained for LacZ. More than 90% of the Neo^r cells were LacZ positive after infection with either vector. Thus, the IRES can be used to express LacZ as a downstream gene and to reliably coexpress a reporter gene and a selectable marker.

LacZ–v-Src expression in ovo. Because LacZ and v-Src were efficiently coexpressed from pLZIS in vitro, this vector was selected for tests in ovo. Virus concentrate, derived either from pLZIS or from the LacZ control vector, pLZ10, was injected into embryos at 55 to 70 h of incubation (Hamburger and Hamilton stages 13 to 17). The embryos were recovered, fixed, and stained for LacZ 3 to 6 days after injection (stages 30 to 34 are equivalent to embryonic days 6 to 8 [E6 to E8]).

In initial experiments, we analyzed LacZ-positive cells in the skin because it is simple, thin, and easily examined in whole mount. Clusters of closely spaced LacZ-positive cells were assumed to be clones on the basis of statistical and double-labeled studies that have been detailed elsewhere (13, 45). In vLZ10 (LacZ only)-injected embryos, typical clones were composed of flat, polygonal cells with large central nuclei and relatively scant cytoplasm (Fig. 4a and b); the average number of cells per clone was about 40 at stages 30 to 34. Plastic sections through such clones revealed that the marked cells were well integrated into the epidermis and identified them as typical cells of the basal and peridermal layers (Fig. 4c and d; see Fig. 7 in reference 45 for similar studies of mouse skin). In contrast, most cells in vLZIS (LacZ–v-Src)-marked clones were markedly abnormal: they were large and irregularly shaped and contained multiple LacZ-negative inclusions that might have been vacuoles or supernumerary nuclei generated by disordered cytokenesis (Fig. 4e and f). Sections through these clones showed that the LacZ-positive cells were poorly integrated into the epidermis (Fig. 4g) and frequently seemed to be delaminating from its apical surface (Fig. 4h). In addition the number of cells per clone was greatly reduced when v-Src was present; the average number of cells per vLZIS-marked clone, counting each potential syncytial aggregate as a single cell, was around five at the stages examined. Finally, it is important to note that the incidence of such abnormalities was high: in one set of vLZIS-injected embryos analyzed at stage 30, 14 of 15 clones of skin cells were markedly aberrant. In embryos analyzed at stage 34, about 25% of the clones contained groups of normal-appearing cells, either in isolation or intermingled with abnormal cells, suggesting that expression of v-Src may be reduced or rendered less toxic at later developmental stages (data not shown). Nonetheless, more than 90% of the clones analyzed at this stage contained one or more clearly aberrant cells. Thus, at least some progeny of most LacZ-positive vLZIS-marked epidermal cells infected in ovo expressed sufficient levels of v-Src to perturb normal developmental processes.

In addition to skin, we dissected and examined the central nervous system of vLZIS-injected embryos. Only a few clones of LacZ-positive cells were found within the brain or spinal cord, and these will be described elsewhere. In roughly 50% of the embryos, however, we found aggregates of LacZ-positive cells in association with the meninges that ensheath the brain and spinal cord and with the loose mesenchyme that overlies the meninges. Examples from the lumbar segments of the spinal cord and from the optic tectum of the mesencephalon are shown in Fig. 5. In both areas, the LacZ-positive cells were heterogeneous in size and shape but were not grossly abnormal in morphology. Most striking, however, was the large size of the clones: each cluster contained hundreds to thousands of LacZ-positive cells. No comparably large clones of meningeal or mesenchymal cells were seen in vLZ10-injected embryos (data not shown), nor have we seen such clones in previous studies of cell lineage in optic tectum (13, 16, 18) or spinal cord (29). From these results, we conclude that vLZIS promotes coexpression of LacZ and v-Src in mesenchymal tissue as well as in skin.

DISCUSSION

The aim of this work was to construct a recombinant retroviral vector which would allow efficient coexpression of two genes in single infected cells. We have shown that use of the EMCV IRES to produce a bicistronic message provides a more efficient means of expressing two genes within individual cells than does use of two promoters or a regulated-splicing mechanism.

Retroviral vectors containing internal promoters are often compromised by the problem of promoter interference, which is dependent on the strength of the promoter and the context in which it is placed. Cullen et al. (4) showed that expression of the preproinsulin gene from the 3′ LTR of the avian leukosis virus occurred only when the upstream LTR was inactivated. This phenomenon was called transcriptional interference and is reminescent of a more natural case observed in avian leukosis virus-induced bursal tumors (38, 41). Such tumors have been associated with insertion of the virus upstream of *c-myc*. In most of these tumors, the provirus was found to bear mutations near its 5′ end that were correlated with expression of *c-myc* from the 3′ LTR (14). Independently, Emmerman and Temin (8, 9) showed that in a double-promoter spleen necrosis virus vector, one gene is usually suppressed when there is selection for the other, regardless of the position of the genes relative to each other. This suppression was found to be epigenetic, reversible, and *cis* acting. It was attributed to a change in chromatin conformation near the active promoter, which in turn inhibited transcription from nearby promoters. More recently, Hoeben et al. (20) have suggested that suppression is associated with methylation and is dependent on the site of integration of the virus. This, however, was not observed by Emmerman and Temin (8).

Different problems occur when splice acceptor sites are used to construct double-expression vectors. If the aim were to produce maximal levels of both gene products, optimal expression would be reached when half of the RNA is spliced. Thus, each gene would be expressed at only 50% of the level expected if no splicing occurred. In addition, the amount of genomic RNA available for packaging, and potentially the viral titer, would be reduced by half. Finally,

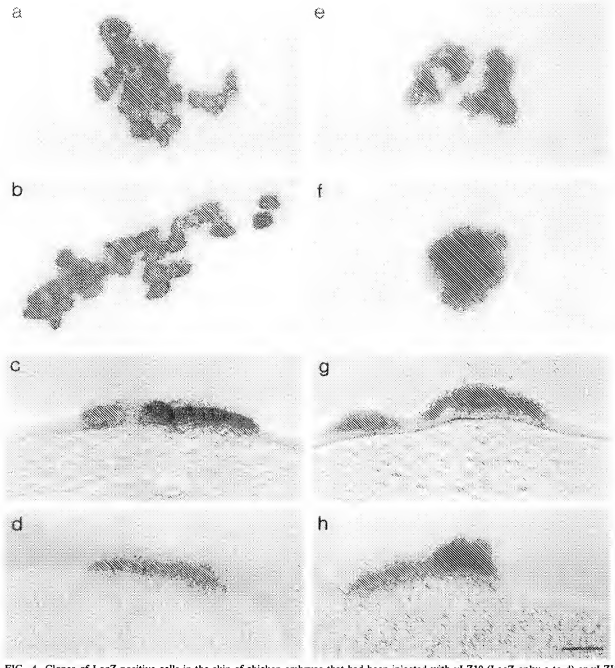

FIG. 4. Clones of LacZ-positive cells in the skin of chicken embryos that had been injected with vLZ10 (LacZ only; a to d) or vLZIS (LacZ–IRES–v-Src; e to h). Embryos were injected on E3 and examined on E6 to E8. (a, b, e, and f) Whole mounts, photographed with bright field optics; (c, d, g, and h) plastic sections photographed with Nomarski optics. Aberrant morphology of LacZ-positive, vLZIS-marked cells demonstrates that these cells express v-Src. The bar represents 50 μm.

regulation of alternative splicing is not well understood in any system, and it is already clear that splicing efficiency in RSV is context dependent and that discrete intronic sequences are responsible for the regulation of splicing (1, 2, 25, 48, 49). Thus, it is not currently possible to engineer vectors that produce spliced and unspliced RNAs in predictable ratios. In addition, for RSV the translational start site for *gag* is retained in the spliced message and could interfere with translation from the AUG of the downstream gene.

To obviate the problems encountered with the double-expression vectors that use internal promoters or regulated splicing, we tested the EMCV IRES. In the vectors that we

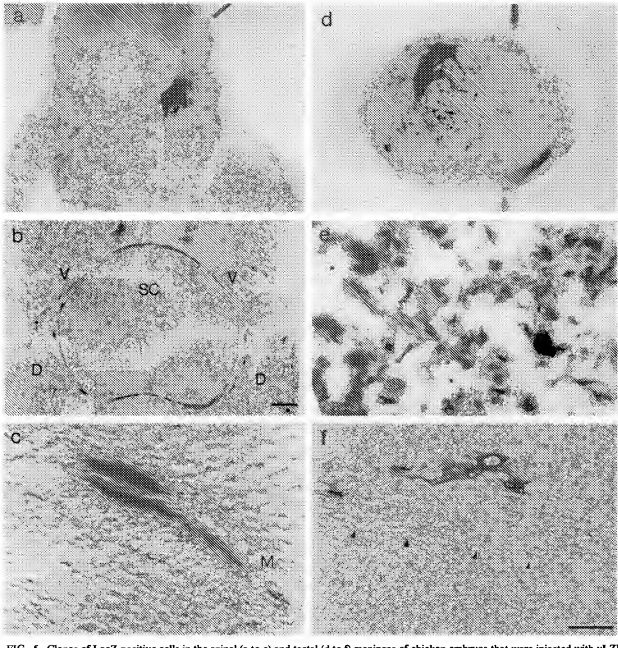

FIG. 5. Clones of LacZ-positive cells in the spinal (a to c) and tectal (d to f) meninges of chicken embryos that were injected with vLZIS on E3 and examined on E8. (a) Large clone of cells surrounding and extending laterally from the spinal cord. (b) Photomontage of a section through vertebral column shows that LacZ-positive cells ensheath but do not penetrate the spinal cord (SC) and extend into mesenchyme surrounding vertebral bodies (V) and dorsal root ganglia (D). Groups of LacZ-positive mesenchymal cells more distant from the cord were also present in this clone but are not visible in this field. (c) At higher power and with Nomarski optics, some of the perispinal cells are seen to be associated with the meninges (M) external to a fiber tract in the spinal cord. (d) Clone of LacZ-positive cells on the surface of the optic tectum. (e) At higher power in whole mount, the cells seem to be disordered, heterogeneous in shape, and numerous. (f) Section photographed with Nomarski optics showing LacZ-positive meningeal cells external to the apical surface (arrowheads) of the tectum. The bar represents 1 mm in panel a, 125 μm in panel b, and 50 μm in panel c, e, and f, and 0.5 mm in panel d.

constructed, both genes were expressed from the 5′ LTR of RSV and translation of the downstream gene in the dicistronic message occurred by ribosomes binding internally to the IRES. The efficiency of translation of the second cistron in such dicistronic mRNAs has been shown to be similar to that of the corresponding gene in a monocistronic message, indicating that interference does not occur at the translational level (23). Several lines of evidence presented here

indicate that the IRES provides the best available method for coexpressing two genes from a retroviral vector. (i) In a population of infected cells grown under no selection, more that 90% of cells infected with an IRES vector coexpressed LacZ and CAT, whereas most cells infected with an internal promoter vector expressed either one gene or the other. (ii) Similarly, coexpression of LacZ and v-Src in infected QT6 cells was also substantially more efficient from the IRES vector than from either an internal promoter or a regulated splicing vector. (iii) The IRES vector permits reliable coexpression of Neo^r and LacZ (>90%) in either order (Neo^r-IRES-LacZ or LacZ-IRES-Neo^r). (iv) The levels of expression of LacZ, CAT, and v-Src determined either by enzymatic assays or by visual inspection of immunostained cells were high. (v) For both LacZ-CAT and LacZ–v-Src vectors, LacZ titers were consistently higher with the IRES vectors. Together, these results provide strong evidence that the EMCV IRES is more efficient than either of the previously used approaches at coexpressing two genes from a recombinant provirus.

We chose the LacZ–IRES–v-Src vector (pLZIS) for injection into embryos because previous studies in vivo and in vitro (26, 30, 42, 46, 47), as well as our observations on cultured cells (Fig. 3), suggested that expression of v-Src would be likely to affect cellular morphology. Indeed, in both skin and meninges, vLZIS-marked cells were consistently different from vLZ10-marked cells in number or size, indicating that most LacZ-positive cells also expressed v-Src. In addition, although our aim was not to study the biology of v-Src, these experiments provide new data on the effects of v-Src on cells in complex tissue. First, expression of v-Src appears to block the normal proliferation of epidermal cells. This inhibition might result either from a general toxic effect of the oncogene or from a more specific interference with endogenous mechanisms of growth control; we cannot distinguish between these alternatives. Our results are somewhat different from those of Stoker et al. (46), who saw disturbances of growth control in only one of several clones of epidermal cells marked by a LacZ–v-Src vector. One possible explanation for the difference is that Stoker et al. used a regulated splicing vector in which many LacZ-positive cells (about 40%) did not express detectable levels of v-Src, and other cells may have expressed lower levels than occur in vLZIS-infected cells. In addition, whereas we analyzed clones at E6 to E8, Stoker et al. did not examine tissue until E12 to E14, by which time v-*src*-poisoned cells might have died and only unaffected cells survived. In contrast, expression of v-Src appears to cause loss of proliferative control in the mesenchyme and meninges. This result is consistent with the known ability of v-*src* to transform mesenchymal cells (e.g., fibroblasts) in vitro and to induce fibrosarcomas in vivo (42). The large clones of mesenchymal and meningeal cells that we observed might have eventually formed tumors, as has been observed previously following infection with replication-defective v-*src*-containing virus (47); however, we confined our observations to short times (3 to 6 days) after infection.

IRES-based retroviral vectors of the sort described in this report may be useful for a variety of purposes. (i) Vectors encoding the LacZ marker and a second bioactive gene can be used to generate small clones of transgenic cells in a wild-type environment. As shown here for vLZIS, the transgenic cells can be identified histochemically, and the effects of the second gene can be assessed by analyzing the phenotype of the labeled cells. (ii) The LacZ-Neo^r vector can be used in transcription activation studies: mutations are introduced in a promoter, Neo^r clones are isolated, and the effect of the mutation on promoter activity is measured by LacZ assays (13a). (iii) Similarly, if vectors for gene therapy were constructed by linking *neo* and the gene of interest by an IRES, selection for G418 resistance should ensure expression of the second gene. Finally, it is important to note that use of the IRES strategy described here is not limited to retroviral vectors. For example, transgenic mice expressing a marker gene (e.g., *lacZ*) and a bioactive gene from a single promoter would allow direct correlation of patterns of transgenic expression with patterns of transgenic effect.

ACKNOWLEDGMENTS

We thank Anne Palmenberg for pE5LVP0, Henry Huang for the CAT fragment with the altered initiation codon, Jeff Milbrandt for the CMV promoter fragment, Robin Morris-Valero and Jeanette Cunningham for technical assistance, Deni Galileo for advice on immunohistochemistry, and Grace Gray for helpful comments.

This work was supported by grants from the McKnight Foundation and NIH to J.R.S. and from NIH to J.E.M.

REFERENCES

1. **Arrigo, S., and K. Beemon.** 1988. Regulation of Rous sarcoma virus RNA splicing and stability. Mol. Cell. Biol. 8:4858–4867.
2. **Berberich, S. L., and M. Stoltzfus.** 1991. Mutations in the region of the Rous sarcoma virus 3′ splice sites: implications for regulation of alternative splicing. J. Virol. 65:2640–2646.
3. **Boshart, M., F. Weber, G. Jahn, K. Dorsch-Hasler, B. Fleckenstein, and W. Schaffner.** 1985. A very strong enhancer is located upstream of an immediate early gene of human cytomegalovirus. Cell 41:521–530.
4. **Cullen, B. R., P. T. Lomedico, and G. Ju.** 1984. Transcriptional interference in avian retroviruses—implications for the promoter insertion model of leukaemogenesis. Nature (London) 307:241–245.
5. **Czernilofsky, A. P., A. D. Levinson, H. E. Varmus, J. M. Bishop, E. Tischer, and H. Goodman.** 1983. Correction to the nucleotide sequence of the src gene of Rous sarcoma virus. Nature (London) 301:736–739.
6. **DeLorbe, W. J., P. A. Luciw, H. M. Goodman, H. E. Varmus, and J. M. Bishop.** 1980. Molecular cloning and characterization of avian sarcoma virus circular DNA molecules. J. Virol. 36:50–61.
7. **Elroy-Stein, O., T. R. Fuerst, and B. Moss.** 1989. Cap-independent translation of mRNA conferred by encephalomyocarditis virus 5′ sequence improves the performance of the vaccinia virus/bacteriophage T7 hybrid expression system. Proc. Natl. Acad. Sci. USA 86:6126–6130.
8. **Emmerman, M., and H. M. Temin.** 1984. Genes with promoters in retrovirus vectors can be independently suppressed by an epigenetic mechanism. Cell 39:459–467.
9. **Emmerman, M., and H. M. Temin.** 1986. Quantitative analysis of gene suppression in retrovirus vectors. Mol. Cell. Biol. 6:792–800.
10. **Foecking, M. K., and H. Hofstetter.** 1986. Powerful and versatile enhancer-promoter unit for mammalian expression vectors. Gene 45:101–105.
11. **Frank, E., and J. R. Sanes.** 1991. Lineage of neurons and glia in chick dorsal root ganglia: analysis *in vivo* with a recombinant retrovirus. Development 111:895–908.
12. **Friedmann, T.** 1989. Progress toward human gene therapy. Science 244:1275–1281.
13. **Galileo, D. S., G. E. Gray, G. C. Owens, J. Majors, and J. R. Sanes.** 1990. Neurons and glia arise from a common progenitor in chick optic tectum: demonstration with two retroviruses and cell type-specific antibodies. Proc. Natl. Acad. Sci. USA 87:458–462.

13a. **Ghattas, I. R., and J. E. Majors.** Unpublished data.

14. **Goodenow, M. M., and W. S. Hayward.** 1987. 5′ long terminal repeats of *myc*-associated proviruses appear structurally intact

but are functionally impaired in tumors induced by avian leukosis virus. J. Virol. 61:2489–2498.
15. **Gorman, C. M., L. F. Moffat, and B. H. Howard.** 1982. Recombinant genomes which express chloramphenicol acetyltransferase in mammalian cells. Mol. Cell. Biol. 2:1044–1051.
16. **Gray, G. E., J. C. Glover, J. Majors, and J. Sanes.** 1988. Radial arrangement of clonally related cells in the chicken optic tectum: lineage analysis with a recombinant retrovirus. Proc. Natl. Acad. Sci. USA 85:7356–7360.
17. **Gray, G. E., S. M. Leber, and J. R. Sanes.** 1990. Migratory pattern of clonally related cells in the developing central nervous system of the chick embryo. Experientia 46:929–940.
18. **Gray, G. E., and J. R. Sanes.** 1991. Migratory paths and phenotypic choices of clonally related cells in the avian optic tectum. Neuron 6:211–225.
19. **Hamburger, V., and H. L. Hamilton.** 1951. A series of normal stages in the development of the chick embryo. J. Morphol. 88:49–92.
20. **Hoeben, R. C., A. A. J. Migchielsen, R. C. M. van der Jagt, H. van Ormondt, and A. J. van der Eb.** 1991. Inactivation of the Moloney murine leukemia virus long terminal repeat in murine fibroblast cell lines is associated with methylation and dependent on its chromosomal position. J. Virol. 65:904–912.
21. **Jakobovits, E. B., J. E. Majors, and H. E. Varmus.** 1984. Hormonal regulation of the Rous sarcoma virus *src* gene via a heterologous promoter defines a threshold dose for cellular transformation. Cell 38:757–765.
22. **Jang, S. K., M. V. Davies, R. J. Kaufman, and E. Wimmer.** 1989. Initiation of protein synthesis by internal entry of ribosomes into the 5′ nontranslated region of encephalomyocarditis virus RNA in vivo. J. Virol. 63:1651–1660.
23. **Jang, S. K., H.-G. Kraussslich, M. J. H. Nicklin, G. M. Duke, A. C. Palmenberg, and E. Wimmer.** 1988. A segment of the 5′ nontranslated region of encephalomyocarditis virus RNA directs internal entry of ribosomes during in vitro translation. J. Virol. 62:2636–2643.
24. **Jang, S. K., and E. Wimmer.** 1990. Cap-independent translation of encephalomyocarditis virus RNA: structural elements of the internal ribosome entry site and involvement of a cellular 57-kd RNA binding protein. Genes Dev. 4:1560–1572.
25. **Katz, R. A., M. Kotler, and A. M. Skalka.** 1988. *cis*-acting intron mutations that affect the efficiency of avian retroviral RNA splicing: implication for mechanisms of control. J. Virol. 62: 2686–2695.
26. **Keller, G., and E. F. Wagner.** 1989. Expression of v-src induces a myeloproliferative disease in bone marrow-reconstituted mice. Genes Dev. 3:827–837.
27. **Kozak, M.** 1989. The scanning model for translation: an update. J. Cell Biol. 108:229–241.
28. **Kriegler, M.** 1990. Gene transfer and expression: a laboratory manual. Stockton Press, New York.
29. **Leber, S. M., S. M. Breedlove, and J. R. Sanes.** 1990. Lineage, arrangement, and death of clonally related motoneurons in spinal cord. J. Neurosci. 10:2451–2462.
30. **Levy, J. B., and J. S. Brugge.** 1989. Biological and biochemical properties of the *c-src*$^{+}$ gene product overexpressed in chicken embryo fibroblasts. Mol. Cell. Biol. 9:3332–3341.
31. **Lopata, M. A., D. W. Cleveland, and B. Sollner-Webb.** 1984. High level transient expression of a chloramphenicol acetyl transferase gene by DEAE-dextran mediated DNA transfection coupled with a dimethyl sulfoxide or glycerol shock treatment. Nucleic Acids Res. 12:5707–5717.
32. **Majors, J., and H. E. Varmus.** 1983. A small region of the mouse mammary tumor virus long terminal repeat confers glucocorticoid hormone regulation on a linked heterologous gene. Proc. Natl. Acad. Sci. USA 80:5866–5870.
33. **Maness, P.** 1986. pp60$^{c\text{-}src}$ encoded by the proto-oncogene *c-src* is a product of sensory neurons. J. Neurosci. Res. 16:127–139.
34. **Miller, A. D., and G. J. Rosman.** 1989. Improved retroviral vectors for gene transfer and expression. BioTechniques 9:980–990.
35. **Miller, J. H.** 1972. Experiments in molecular genetics. Cold Spring Harbor Laboratory, Cold Spring Harbor, N.Y.
36. **Morinaga, Y., T. Franceschini, S. Inouye, and M. Inouye.** 1984. Improvement of oligonucleotide-directed site-specific mutagenesis using double-stranded plasmid DNA. Bio/Technology 2:636–639.
37. **Moscovici, C., G. Moscovici, H. Jimenez, M. M. C. Lai, M. J. Hayman, and P. K. Vogt.** 1977. Continuous tissue culture cell lines derived from chemically induced tumors of Japanese quail. Cell 11:95–103.
38. **Neel, B. G., W. S. Hayward, H. L. Robinson, J. Fang, and S. M. Astrin.** 1981. Avian leukosis virus-mediated tumors have common proviral integration sites and synthesize discrete new RNAs: oncogenesis by promoter insertion. Cell 23:323–334.
39. **Overell, R. W., K. E. Weisser, and D. Cosman.** 1988. Stably transmitted triple-promoter retroviral vectors and their use in transformation of primary mammalian cells. Mol. Cell. Biol. 8:1803–1808.
40. **Parks, G. D., G. M. Duke, and A. C. Palmenberg.** 1986. Encephalomyocarditis virus 3C protease: efficient cell-free expression from clones which link viral 5′ noncoding sequences to the P3 region. J. Virol. 60:376–384.
41. **Payne, G. S., S. A. Courtneidge, L. B. Crittenden, A. M. Fadly, J. M. Bishop, and H. E. Varmus.** 1981. Analysis of avian leukosis virus DNA and RNA in bursal tumors: viral gene expression is not required for maintenance of the tumor state. Cell 23:311–322.
42. **Pimentel, E.** 1989. Oncogenes, 2nd ed., vol. 2, p. 115–158. CRC Press, Boca Raton, Fla.
43. **Price, J., D. Turner, and C. Cepko.** 1987. Lineage analysis in the vertebrate nervous system by retrovirus-mediated gene transfer. Proc. Natl. Acad. Sci. USA 84:156–160.
44. **Sambrook, J., E. F. Fritsch, and T. Maniatis.** 1989. Molecular cloning: a laboratory manual, 2nd ed. Cold Spring Harbor Laboratory, Cold Spring Harbor, N.Y.
45. **Sanes, J. R., J. L. R. Rubenstein, and J.-F. Nicolas.** 1986. Use of a recombinant retrovirus to study post-implantation cell lineage in mouse embryos. EMBO J. 5:3133–3142.
46. **Stoker, A. W., C. Hatier, and M. Bissell.** 1990. The embryonic environment strongly attenuated v-src oncogenesis in mesenchymal and epithelial tissues, but not in endothelia. J. Cell Biol. 111:217–228.
47. **Stoker, A. W., and M. H. Sieweke.** 1989. v-src induces clonal sarcomas and rapid metastasis following transduction with a replication-defective retrovirus. Proc. Natl. Acad. Sci. USA 86:10123–10127.
48. **Stoltzfus, C. M., and S. J. Fogarty.** 1989. Multiple regions in the Rous sarcoma virus *src* gene intron act in *cis* to affect the accumulation of unspliced RNA. J. Virol. 63:1669–1676.
49. **Stoltzfus, C. M., S. K. Lorenzen, and S. L. Berberich.** 1987. Noncoding region between the *env* and *src* genes of Rous sarcoma virus influences splicing efficiency at the *src* gene 3′ splice site. J. Virol. 61:177–184.
50. **Swanstrom, R., W. J. DeLorbe, J. M. Bishop, and H. E. Varmus.** 1981. Nucleotide sequence of cloned unintegrated avian sarcoma virus DNA: viral DNA contains direct and inverted repeats similar to those in transposable elements. Proc. Natl. Acad. Sci. USA 78:124–128.
51. **Swanstrom, R., R. C. Parker, H. E. Varmus, and J. M. Bishop.** 1983. Transduction of a cellular oncogene: the genesis of Rous sarcoma virus. Proc. Natl. Acad. Sci. USA 80:2519–2523.
52. **Temin, H. M.** 1986. Retrovirus vectors for gene transfer: efficient integration into and expression of exogenous DNA in vertebrate cell genomes, p. 149–187. *In* R. Kucherlapati (ed.), Gene transfer. Plenum Press, New York.
53. **van der Eb, A. J., and F. L. Graham.** 1980. Assay of transforming activity of tumor virus DNA. Methods Enzymol. 65:826–839.
54. **Weiss, R., N. Teich, H. E. Varmus, and J. Coffin (ed.).** 1982. RNA tumor viruses. Cold Spring Harbor Laboratory Press, Cold Spring Harbor, N.Y.

EXHIBIT C

Proc. Natl. Acad. Sci. USA
Vol. 93, pp. 5185–5190, May 1996
Medical Sciences

Rapid retroviral delivery of tetracycline-inducible genes in a single autoregulatory cassette

ANDREAS HOFMANN*, GARRY P. NOLAN*†, AND HELEN M. BLAU*‡

*Department of Molecular Pharmacology, and †Department of Microbiology and Immunology, Stanford University School of Medicine, Stanford, CA 94305-5332

Communicated by Anthony P. Mahowald, University of Chicago, Chicago, IL, January 16, 1996 (received for review November 1, 1995)

ABSTRACT **We describe a single autoregulatory cassette that allows reversible induction of transgene expression in response to tetracycline (tet). This cassette contains all of the necessary components previously described by others on two separate plasmids that are introduced sequentially over a period of months [Gossen, M. & Bujard, H. (1992) *Proc. Natl. Acad. Sci. USA* 89, 5547–5551]. The cassette is introduced using a retrovirus, allowing transfer into cell types that are difficult to transfect. Thus, populations of thousands of cells, rather than a few clones, can be isolated and characterized within weeks. To avoid potential interference of the strong retroviral long terminal repeat enhancer and promoter elements with the function of the tet-regulated cytomegalovirus minimal promoter, the vector is self-inactivating, eliminating transcription from the long terminal repeat after infection of target cells. Tandem tet operator sequences and the cytomegalovirus minimal promoter drive expression of a bicistronic mRNA, leading to transcription of the gene of interest (*lacZ*) and the internal ribosome entry site controlled transactivator (Tet repressor–VP16 fusion protein). In the absence of tet, there is a progressive increase in transactivator by means of an autoregulatory loop, whereas in the presence of tet, gene expression is prevented. Northern blot, biochemical, and single cell analyses have all shown that the construct yields low basal levels of gene expression and induction of one to two orders of magnitude. Thus, the current cassette of the retroviral construct (SIN-RetroTet vector) allows rapid delivery of inducible genes and should have broad applications to cultured cells, transgenic animals, and gene therapy.**

Studies of gene function in cultured cells, analyses of gene expression during mammalian development, and delivery of proteins via gene therapy would all greatly benefit from the ability to regulate gene expression in a temporal and quantitative manner. In cultured cells, a frequent approach to the study of genes is stable transfection of plasmids and isolation of constitutively expressing cells using a drug selectable marker, a procedure that is time consuming, labor intensive, and may result in loss of function of the gene of interest over time. In mouse development, the role of genes is typically studied by irreversible changes: for example, gene inactivation or gene augmentation in transgenic animals from the onset of embryogenesis or use of *flp* or *cre* recombinases later in development (1, 2). In gene therapy, only constitutive delivery of proteins has been achieved, yet constant expression levels are often not physiological and can even be life threatening. In each of these three cases, it would be highly advantageous if the gene of interest could be expressed during a particular window of time in a dose-dependent and reversible manner.

Several inducible gene expression systems have been developed over the past decade in an attempt to meet the need for regulated gene expression. Most of the commonly used methods for inducing gene expression such as heat shock, steroids, or metallothionein, suffer from either high basal levels of gene expression under noninduced conditions, pleiotropic effects on host cell genes, or both (reviewed in refs. 3 and 4). Although usefully applied in a multitude of studies over the past decade, these inducible systems are fraught with problems.

Recently two systems have been developed that appear to overcome many of the problems associated with the first generation of inducible vectors in that the inducers are specific to the gene of interest and lead to low basal and high inducible levels of gene expression: the tetracycline (tet) and progesterone antagonist (RU486) regulatable systems (5, 6). Both systems use microbial proteins and microbial DNA response elements to drive the expression of a desired gene in heterologous cells. As a result, regulation is restricted to the gene of interest, host genes are not affected, and there appears to be no associated toxicity. In addition, gene expression can frequently be modulated over a broad range of levels during a defined temporal window.

The two-plasmid systems described above (5, 6), represent theoretical milestones in the development of inducible systems, yet widespread application is severely hindered for several reasons. First, two sequential transfection steps are necessary to introduce each of the two plasmids stably, requiring several months in order that individual clones be tested at each step. Second, use in poorly transfectable cell types such as primary myoblasts or lymphocytes remains difficult. Thus, in practice, obtaining well-regulated clones using the two-plasmid systems is not only limited to certain cell types, but is also cumbersome, labor intensive, and low in yield of inducible clones.

To overcome these problems, we developed a single cassette that contains all of the components required for tet regulation. In this report, the cassette is contained in a retrovirus, which can be produced at high titer and infects dividing cells with high efficiency, allowing use in a large number of cell types. The retrovirus requires minimal effort to prepare, is stable, and can yield populations of cells with regulatable gene expression within weeks, instead of months. The potential problem of cis-regulatory effects due to the close proximity of the tet-regulatable cytomegalovirus (CMV) minimal promoter elements to strong viral regulatory elements has been circumvented by utilizing a self-inactivating (SIN) retroviral vector (7). Following infection of the target cell, the SIN vector, which contains a deletion in the enhancer and promoter sequences of the 3′ long terminal repeat (LTR), transfers this deletion to the 5′ LTR, resulting in transcriptional inactivation of the provirus. As a result, the tet-regulatable minimal promoter drives expression of a bicistronic mRNA encoding the gene of interest and an internal ribosome entry site (IRES) (8) controlled transactivator. In the presence of tet, the low levels of transactivator transcribed are effectively inhibited from binding the tet operator sequences due to allosteric changes, whereas in the absence of tet, the transactivator promotes its

The publication costs of this article were defrayed in part by page charge payment. This article must therefore be hereby marked "*advertisement*" in accordance with 18 U.S.C. §1734 solely to indicate this fact.

Abbreviations: tet, tetracycline; Dox, doxycycline; CMV, cytomegalovirus; SIN, self-inactivating; IRES, internal ribosome entry site; LTR, long terminal repeat; β-gal, β-galactosidase; FACS, fluorescence-activated cell sorter.

‡To whom reprint requests should be addressed.

own transcription in an autoregulatory loop, reaching a plateau when all operator sequences are presumably occupied. Due to its rapid introduction into large numbers of primary cells, potential for analyses of gene expression shortly after introduction, and broad host cell range, the retroviral vector has all of the positive attributes of the original two-plasmid tet regulatable system, while being much more amenable to use in a variety of contexts.

MATERIALS AND METHODS

Vector Construction. All cloning steps were performed as described (9). For the vector backbone pBABE M *lacZ*, a pBABE based retroviral vector (10) bearing the MFG packaging signal Moloney murine leukemia virus was used (S. Kinoshita and G.P.N., unpublished data). Vectors bearing the elements of the tet-regulatable system including the minimal human CMV promoter, tet repressor VP16 fusion protein (transactivator), and tet operator sequences were gifts from H. Bujard (5). The IRES was derived from Mengo virus (gift of J. P. Morgenstern, Mellenium Corporation). The final vector construct was named pBABE SIN CMV 15–1 (SIN-RetroTet vector). To construct a SIN vector, the 3′ LTR of pBABE M *lacZ* was exchanged with the mutant 3′ LTR of pJ1Pro$^-$ (gift of R. Mulligan, Whitehead Institute, Massachusetts Institute of Technology), which lacks the promoter and enhancer sequences in the 3′ LTR.

Cell Culture. Primary mouse myoblasts (C57BL/6) were purified earlier (11). Cells were grown in myoblast growth medium consisting of 50% F10 medium (GIBCO/BRL) and 50% DMEM (GIBCO/BRL), supplemented with 20% fetal bovine serum (HyClone), basic fibroblast growth factor (2.5 ng/ml; Promega), penicillin G (200 units/ml), and streptomycin (200 μg/ml). Cells were grown on collagen-coated dishes (Sigma) in a humidified 5% CO_2 incubator at 37°C. tet (Sigma) and doxycycline (Dox) (Sigma) were stored at −20°C in the dark as 1 mg/ml stock solutions in 30% ethanol and 50% ethanol, respectively, and added to the medium as needed.

β-Galactosidase (β-gal) Assays. *Cell lysates.* β-gal activity was measured with 1 μg of protein using the Galacto-Light Plus kit (Tropix, Bedford, MA) according to the specifications of the manufacturer. For these chemiluminescence assays, cells were grown on 60-mm tissue culture plates for 2–3 days until they reached 70–80% confluency. At that time, cells were harvested and assayed by integration for 10 sec with a Monolight 2001 luminometer. All samples were measured twice and the mean value was corrected for the background activity of the assay (10 μl of lysis buffer), which varied in different experiments between 900 and 3000 relative light units.

Fixed cells. Staining of cells for β-gal expression on culture dishes was performed as described (12).

Live cells. β-gal expression in living cells was determined by fluorescence-activated cell sorting (FACS) as described (13) except that the fluorescein di-β-D-galactopyranoside (FDG) concentration was reduced to 0.5 mM to reduce the background signal seen with 2 mM (unpublished observations).

Transfection of BOSC23 Cells and Transduction of C57BL/6 Primary Myoblasts. Retroviral particles were obtained after transient transfection of BOSC23 cells as described (14). The viral supernatant was collected and either was used immediately for transductions or was frozen on dry ice, stored at −80°C, and used in later transductions. Primary myoblasts (5×10^5) (C57BL/6) were plated 1 day prior to transduction, and just before transduction, myoblast growth medium was removed and replaced with undiluted viral supernatant supplemented with 8 μg/ml Polybrene. In general, cells were incubated overnight at 32°C in a humidified 5% CO_2 incubator. The viral supernatant was then aspirated and cells were transferred to myoblast growth medium and growth conditions. Cells were then either expanded or assayed for β-gal activity 48 hr posttransduction.

Northern Blot Analysis. Northern blotting was performed as described (15) using a digoxigenin-labeled probe (approximately 2 kb), complementary to the *lacZ* gene. The bound probe was visualized by chemiluminescence using CSPD substrate (Tropix) at a final concentration of 0.1 mg/ml.

RESULTS

Design of the tet-Regulatable Retroviral Vector. In the tet system of Gossen and Bujard (5), a first plasmid constitutively expresses a transactivator, a fusion protein between the tet repressor (TetR) and the transcriptional activation domain of the herpes simplex virus VP16 protein. On a second plasmid is the heptamerized tet operator (TetO) sequence followed by a human CMV immediate early minimal promoter ($P_{hCMV*-1}$) and the gene of interest.

The retroviral construct shown in Fig. 1 was designed to contain all of these components as follows. To achieve low basal levels of expression of the gene of interest and of the transactivator, the relatively weak $P_{hCMV*-1}$ promoter was used. Low promoter activity leads to the transcription of an mRNA that is initiated upstream of the gene of interest (in this case, the *lacZ* gene), progresses through the transactivator sequence, and terminates at the polyadenylylation site located in the R region of the viral 3′ LTR. Thus, a bicistronic mRNA is produced coding for β-gal and an IRES controlled transactivator. As a result, translation ceases downstream of the stop codon of the gene of interest (*lacZ*) in the IRES-

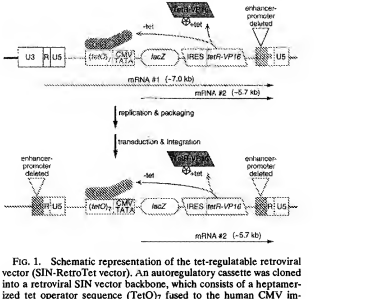

FIG. 1. Schematic representation of the tet-regulatable retroviral vector (SIN-RetroTet vector). An autoregulatory cassette was cloned into a retroviral SIN vector backbone, which consists of a heptamerized tet operator sequence $(TetO)_7$ fused to the human CMV immediate early minimal promoter (CMV TATA) designated $P_{hCMV*-1}$. Upon infection of target cells (myoblasts), the basal activity of the $P_{hCMV*-1}$ promoter drives the expression of a bicistronic mRNA (mRNA 2) with a calculated length of approximately 5.7 kb, coding for β-gal (*lacZ* gene) and the IRES-controlled tet repressor-VP16 fusion protein (TetR-VP16). In the presence of tet, the TetR-VP16 does not bind the TetO sequences, and expression levels are reduced to those of the basal promoter. In the absence of tet, the binding of the TetR-VP16 to the TetO sequences results in increased expression levels from the $P_{hCMV*-1}$ promoter due to the recruitment of transcription factors by the VP16 transcriptional activation domain. In packaging cells in which the virus is produced, mRNA 1 (≈7.0 kb) and mRNA 2 (≈5.7 kb) are transcribed (*Upper*). Upon infection of the myoblast target cell (*Lower*), the promoter and enhancer elements in the viral 5′ LTR are deleted upon integration into the host genome resulting in transcription of mRNA 2 (≈5.7 kb).

sequence, but is reinitiated at the first ATG at the very 3′ end of the IRES-sequence which mediates translation of a second protein, the transactivator. Like the two-plasmid system of Gossen and Bujard (5), in the presence of tet the transactivator undergoes an allosteric change and does not bind the tet operator sequences leading to a lack of gene expression, whereas in its absence the transactivator binds tightly and gene expression is induced. However, basal transcription is essential for some transactivator molecules to be produced. In the absence of tet, as the concentration of transactivator reaches a necessary threshold, the heptamerized operator sequences are bound, further increasing transcription levels of the bicistronic mRNA until they reach a maximum, at which point gene expression plateaus. Thus, a major difference between the two-plasmid system and the retroviral vector is that induction using the single vector results from an autoregulatory feedback loop.

Other features critical to the design of the retroviral vector are the use of the MFG packaging sequence of pBABE M (S. Kinoshita and G.P.N., unpublished data) and the construction of a SIN retroviral vector (7). The MFG packaging sequence leads to high efficiency incorporation of the vector RNA into the maturing virions (G.P.N., unpublished observation). Due to the high titer of virus produced, it is possible to transduce cells that are difficult to transfect, such as primary myoblasts (Fig. 2) and lymphocytes (unpublished observation). Potential cis-regulatory problems in the tet regulation of the P_{hCMV^*-1} promoter due to proximity to potent Moloney viral enhancer and promoter elements are eliminated by the use of a SIN vector, which lacks these elements.

FACS-Enrichment for a Population of tet-Regulatable Transduced Primary Myoblasts. The high transduction efficiency characteristic of retroviral vectors allows stable introduction of the inducible gene of interest into a population of cells within a few days. A caveat of all protocols that involve integration of DNA in the genome is that the expression of the gene of interest may be influenced by its proximity to endogenous promoters, enhancers, or silencers, leading to constitutive gene expression or lack of expression. Because the likelihood of a vector integrating next to such a region within the host genome increases with the number of integrations per cell, transductions were performed under conditions that resulted in approximately 10% efficiency, a frequency that should statistically yield, at most, one viral integration per genome. The actual transduction efficiency was determined as β-gal expression in the absence of tet by X-gal staining assessed at the single-cell level by microscopy. For this purpose, three randomly selected fields were scored containing approximately 2000 cells per field and an average of 240 cells per field stained blue in the absence of tet in accordance with the predicted frequency. Under these conditions, the viral titer was approximately 1.6×10^4 infectious particles per ml. There was a range of β-gal expression. Some of the cells exhibited basal levels of expression that could be detected by X-gal staining even in the presence of tet, whereas others did not. Upon tet removal, the majority of the transduced cells could be induced to express at least one to two orders of magnitude greater levels of β-gal (see below).

To isolate a more uniform population of cells with particularly low basal and high inducible levels of gene expression, the FACS was used, which allows isolation of live transduced cells en masse (Fig. 2*A*). After transduction, primary myoblasts were first grown in a medium that contained the tet analogue Dox (1 μg/ml) for 5 days and cells that exhibited levels of β-gal indistinguishable from untransduced control cells were collected. After expansion and growth without Dox for one week, the myoblasts were reanalyzed by FACS. Cells with approximately 1 order of magnitude higher levels of β-gal activity than untransduced control cells were collected. Following two rounds of FACS sorting after growth without Dox and collection of β-gal expressing cells using similar fluores-

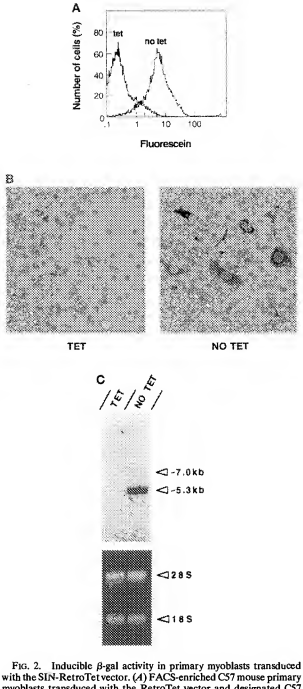

FIG. 2. Inducible β-gal activity in primary myoblasts transduced with the SIN-RetroTet vector. (*A*) FACS-enriched C57 mouse primary myoblasts transduced with the RetroTet vector and designated C57 BABE SIN CMV 15-1 were grown either in the presence (tet) or absence (no tet) of 0.1 μg/ml tet for 4 days and analyzed by FACS. As shown in the histogram of number of cells (%) (ordinate) and log fluorescein (abscissa) gene expression is induced in the majority of cells. (*B*) At the single-cell level, X-gal staining and microscopic analysis of this population revealed no blue cells under noninduced conditions (tet) but almost 100% blue cells upon induction (no tet). (*C*) Northern blot analyses were carried out for C57 BABE SIN CMV 15-1 cells grown either in the presence (tet) or absence (no tet) of 1 μg/ml tet for 2 days. Total RNA (10 μg) was separated on a 1% agarose gel and probed with a digoxigenin-labeled riboprobe complementary to the *lacZ* DNA (*Upper*). Only under induced conditions (no tet), a band of ≈5.3 kb (calculated based on the migration of the 18S and 28S rRNA) was visible approximating the expected size of mRNA 2. The ethidium bromide staining of the same gel (*Lower*) shows that equal amounts of RNA were loaded per lane.

cence gate=, more than 90% of the isolated cell population exhibited regulatable β-gal expression (Fig. 2*A*). This population of regulatable transduced myoblasts, referred to as C57 BABE SIN CMV 15-1, remained stable in its inducible properties for 2 months as determined by FACS and by X-gal staining (Fig. 2 *A* and *B*) and was used in all subsequent experiments described below.

To test whether the retroviral vector acts as a SIN vector upon myoblast infection, Northern blot analysis (Fig. 2*C*) of C57 BABE SIN CMV 15–1 myoblasts was carried out. In RNA from uninduced cells (+tet) no transcript was evident. After long exposures a transcript was barely detectable at ≈5.3 kb, but never at ≈7.0 kb (data not shown), providing evidence that transcription was driven by the CMV promoter and that the viral 5′ LTR was nonfunctional. The major band evident in the absence of tet (−tet) approximates the expected size of ≈5.7 kb. The faint higher molecular weight transcripts are likely to be read-through products or result from activation of a cryptic promoter(s). Thus, Northern blot analysis confirmed that the vector results in a low basal level of mRNA expression, and that the fold induction in the absence of tet is relatively high.

Regulation of *lacZ* Gene Expression Assessed by Chemiluminescence. We compared the properties of the new single-vector retroviral system with the previously described two-vector plasmid system (5) in the C57 BABE SIN CMV 15-1 myoblast population. In a preliminary experiment a chemiluminescence assay was used to determine β-gal activity biochemically. When the background levels for four replicate plates of untransduced myoblasts were substracted from the values for C57 BABE SIN CMV 15-1 cells grown either continuously in tet for 2 days or grown continuously in the absence of tet, a 600-fold induction was observed.

The dose-response curve for β-gal activity in the presence of different concentrations of tet and its analog Dox was determined using a chemiluminescence assay (Fig. 3). For this purpose C57 BABE SIN CMV 15-1 cells were plated in replicate dishes and grown in the absence of tet or Dox for one day, after which the indicated amounts of either tet or Dox were added to the medium. At 70 to 80% cell confluency, or 60 hr after the addition of tet or Dox, cells were harvested and β-gal activities measured in cell lysates by chemiluminescence assays. The mean value for each dose of antibiotic obtained in duplicate dishes was determined as indicated in Fig. 3, which shows a representative of two independent experiments. At a tet concentration of 5 ng/ml, β-gal activity was reduced to basal levels whereas only 50 pg/ml of Dox was sufficient to prevent *lacZ* gene expression. At the antibiotic concentrations used, no toxicity was observed, assayed as changes in cell morphology or viability. Both the dose response curve and greater potency of Dox agree well with results reported using the two-plasmid transfection system (5, 16).

To determine the kinetics of inactivation and activation of gene expression, β-gal activity was assessed in replicate dishes after addition or withdrawal of tet, respectively (Fig. 3 *lower*). Addition of tet led to an average reduction of β-gal activity to 50% of levels of maximally expressing control cells within 8 hr, and basal levels after 48 hr. The kinetics of induction were slower. Twenty-four hours after tet removal only a slight increase in β-gal activity was detectable, but that level approximated maximal levels by 48 hr. Clearly with this vector the loss of *lacZ* gene expression is faster than the induction of gene expression.

Single-Cell Analysis of Kinetics of Induction of *lacZ* Gene Expression by FACS. To determine whether the increase in β-gal activity seen between 24 and 48 hr was due to a few cells rapidly reaching maximal β-gal activities or to the concerted action of the entire population, C57 BABE SIN CMV 15-1 cells were analyzed by FACS at various time points after tet removal (Fig. 4). The histograms obtained for β-gal activity in this population 24 hr after removal of tet were largely coincident with the histograms obtained for cells that were not transduced with the retroviral vector (*Top*). A significant shift toward higher β-gal activity had occurred by 48 hr and this increase was characteristic of the entire FACS sorted population (*Middle*). By 72 hr, maximal induction of gene expression was observed in that the histogram for the induced population was coincident with that of positive controls never exposed to tet. These properties were characteristic of the population even after a period of 2 months. Thus, with this particular gene, by two independent quantitative assays (chemiluminescence and FACS), basal levels of the entire cell population were low and then increased one to two orders of magnitude when the inhibitor was removed, an induction which should suffice for most biological applications.

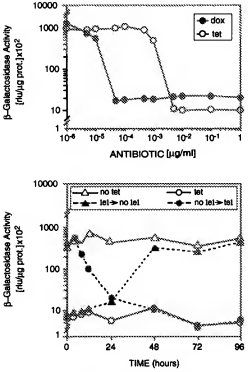

FIG. 3. Pharmacologic properties of regulation of β-gal expression in primary mouse myoblasts transduced with the SIN-RetroTet vector. (*Upper*) Dose-response to tet and Dox. C57 BABE SIN CMV 15-1 cells were grown in the presence of different tet and Dox concentrations, respectively, and β-gal activities in cell lysates were determined after 60 hr by chemiluminescence. A representative of two independent experiments, each performed in replicate, is shown with a maximal difference among measurements of 15%. Low concentrations of 50 pg/ml of Dox and 5 ng/ml of tet were sufficient to reduce β-gal activities to basal levels. (*Lower*) Reversability of gene expression: kinetics of induction and de-induction. C57 BABE SIN CMV 15-1 cells were grown either in the presence or absence of 0.1 μg/ml of tet for 4 days. At time 0, cells which were grown in the presence of tet were washed with PBS and grown in tet-free medium (▲ tet → no tet). Cells grown in the absence of tet were also washed with PBS and then grown in medium containing tet (● no tet → tet). Control cells were grown either continuously in the absence of tet (Δ no tet) or continuously in the presence of tet (○ tet). β-gal activity in cell lysates was measured for duplicate dishes by chemiluminescence (rlu, relative light units) at the time points indicated and the mean values were plotted. Eight hours after tet addition (●) β-gal activities were reduced to approximately 50% of minimal levels (○). Cells in which gene expression was induced (▲) approached β-gal activities of control cells (Δ) after 48 hr and were equivalent to control levels within 96 hr.

DISCUSSION

The single retroviral vector described in this report extends the use of the elegant tet system developed by Gossen and Bujard

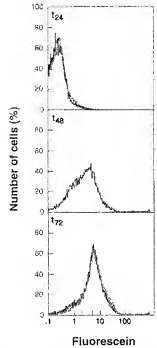

FIG. 4. Reversibility of gene expression by FACS analyses of the population of primary myoblasts expressing the SIN-RetroTet vector. C57 BABE SIN CMV 15-1 cells were grown in the presence of 0.1 μg/ml of tet, and at time 0 hr, cells were washed with PBS and grown in tet-free medium. At different time points the population was analyzed by FACS and plotted as a histogram as the percent of cells (ordinate) and log fluorescein (abscissa). Whereas 24 hr after induction (t_{24}) the induced population (blue) exhibited background activity and was essentially indistinguishable from untransduced C57 primary myoblasts (red), after 48 hr (t_{48}) the entire population had shifted to express β-gal as reflected by higher fluorescein values. By 72 hr after induction (t_{72}), the induced population (blue) was indistinguishable from constitutively induced C57 BABE SIN CMV 15-1 cells (red) and expressed maximal β-gal levels.

(5) to allow widespread regulatable transgene expression *in vitro* and *in vivo* in a manner not possible using that original system (5). The Gossen and Bujard two-vector system requires the stable transfection of first one and then another plasmid, a procedure that is both cumbersome and time consuming, requiring months for the selection and testing of individual clones at each step. By contrast, use of the tet-regulatable retroviral vector described here allows rapid (within weeks) isolation and characterization of large numbers of cells ($>10^4$) that exhibit regulated gene expression. This is advantageous since a population of cells is more representative than a few carefully selected clones for analysis of gene expression. Individual clones may differ from one another and may fluctuate after long-term propagation. Indeed, one or both of the two tet-regulated plasmids ceased to be expressed or was eliminated from myogenic cells over time (S. E. Elson, M. Conboy, H.M.B., unpublished). An added advantage of the retroviral vector described here for regulated gene expression is that retroviruses generally integrate as a single copy into the genome of the target cell, whereas sequential plasmid transfection can be problematic because the integration of multiple plasmids in tandem can raise basal levels of gene expression. A further advantage is that the virus is easily prepared at high titers and is stable after long-term storage. Due to the MFG packaging sequence of this retroviral vector, it can infect a broad range of primary cells that are not easily transfected, including primary muscle cells and lymphocytes at efficiencies as high as 95 and 40%, respectively (unpublished observations).

To avoid potential effects on tet regulation by the weak minimal CMV promoter due to close proximity to the strong Moloney viral 5′ LTR enhancer and promoter control elements, these retroviral sequences were deleted postinfection resulting in a self-inactivating vector. That the vector was indeed a SIN vector (7) was evident from the size of the mRNA observed on Northern blots, which was the reduced size expected if transcription was driven by the CMV minimal promoter, not the retroviral regulatory sequences in the 5′ LTR. Due to the P_{hCMV^*-1} promoter, transactivator production was constitutive but low, leading to low basal levels of gene expression. However, in the absence of tet, this finite amount of transactivator was sufficient to act in an autoregulatory loop, binding the heptameric tet operator sequences upstream of the CMV promoter. The progressive accumulation of transactivator presumably resulted in the observed plateau of gene expression, between one to two orders of magnitude above basal levels.

By contrast with previously used inducers of mammalian gene expression, modulation of transgene expression by tet is easily achieved over several orders of magnitude, is specific to the gene of interest, and is not toxic, because of the nonmammalian origin of the control elements and the low doses of regulator used. Other recently developed two-plasmid inducible systems that use microbial regulatory components (6, 17) suffer from the same problems as the original tet system (5), as they have not yet been combined into a single cassette. To capitalize on the power of the FACS to isolate populations of cells that regulate a gene of interest that encodes a gene product that cannot itself be detected by the FACS, further modifications are now being introduced into the vector such as a second IRES followed by a small gene encoding a sortable marker such as the green fluorescent protein (18).

The time course for the decline in β-gal activity with the retroviral vector was significantly shorter than the time course for induction. The kinetics of de-induction depend on the turnover rate of the transcript and the protein it encodes. In this case, the t_{50} was 8 hr, which approximates the half-life of the regulated gene product, β-gal (G.P.N., unpublished observation). For a gene that has a shorter half-life of either its encoded mRNA or protein, loss of gene expression may be more rapid. By contrast with the kinetics of de-induction, the kinetics of induction of gene expression were relatively slow. The kinetics of induction of the current retroviral vector are presumably due to the autoregulatory nature of the vector that requires multiple rounds of transcription to reach a maximum level of transcription. Other inducible retroviral constructs are being developed that may overcome this limitation and activate gene expression more rapidly (A.H. and H.M.B., unpublished).

In cultured cells, there are numerous potential applications of inducible retroviral vectors. Studies of gene products deleterious to the growth of cells such as cell cycle regulators or tumor suppressors have largely been restricted to analysis by transient transfection or inducible regulation in yeast. The retroviral vector described here may advance these studies by allowing induction and de-induction of expression of such regulators in the same stably infected populations of mammalian cells in a manner previously not possible.

In mice, the ability to induce gene expression reversibly and to modulate the levels of the gene product of interest over time is not currently possible. Regulated gene expression should be of great utility, especially when overexpression or inactivation of the gene of interest results in embryonic lethality. Although site-specific recombinases can target activation or inactivation of gene expression at later times in development (1, 2), they are not dose-dependent or reversible. Since the two-plasmid system functions when naked DNA is directly injected into the

muscles of mice (19), the cassette present in the retroviral vector described here is likely also to be regulated in a dose-dependent manner *in vivo*. Transgenic animals that express tet-inducible reporter genes have been successfully produced by mating transgenic animals into which one or the other of the two plasmids was introduced in one-cell embryos (20, 21). The tet-regulatable cassette described here could be introduced into fertilized cells producing transgenic animals in a single step thereby precluding the need for raising and breeding mice containing single plasmids in order to obtain progeny in which both plasmids are present and the gene of interest is regulated, a time-consuming and expensive undertaking. Furthermore, tet-regulatable cassettes could be used to evade embryonic lethality allowing the generation of mouse models of adult onset human genetic diseases in a manner previously not possible.

For gene therapy, gene delivery that leads to constitutive expression of products such as hormones, neurotrophins, or cytokines is often not physiological and may decrease efficacy or lead to deleterious effects. Typically endogenous expression is regulated or pulsatile. tet-regulated retroviral vectors could be readily delivered to a range of primary cells *ex vivo*, which following implantation *in vivo* could exhibit regulated gene expression. This possibility is presently precluded by the need for successive transfection of plasmids. Thus, both efficacy and safety should be increased by the facility of delivering tet-regulated retroviral vectors that allow modulation of gene expression in gene therapy.

We are grateful to our colleagues in our laboratories for experimental suggestions and critical discussion of the manuscript and to Dr. Hermann Bujard for generously providing us with the tet regulatable two-plasmid system and sharing data pre-publication. A.H. is a recipient of a postdoctoral fellowship from the Deutsche Forschungsgemeinschaft. G.P.N. is a Scholar of the Leukemia Society of America and is supported by National Institutes of Health Grant A135304. This work was supported by research grants from the National Institutes of Health (CA59717 and AG09521), the March of Dimes Birth Defects Foundation, and the Muscular Dystrophy Association to H.M.B.

1. Lakso, M., Sauer, B., Mosinger, B., Jr., Lee, E. J., Yu, S. H., Mulder, K. L. & Westphal, H. (1992) *Proc. Natl. Acad. Sci. USA* **89**, 6232–6236.
2. O'Gorman, S., Fox, D. T. & Wahl, G. M. (1991) *Science* **251**, 1351–1355.
3. Yarranton, G. T. (1992) *Curr. Opin. Biotechnol.* **3**, 506–511.
4. Gossen, M., Bonin, A. L. & Bujard, H. (1993) *Trends Biochem. Sci.* **18**, 471–475.
5. Gossen, M. & Bujard, H. (1992) *Proc. Natl. Acad. Sci. USA* **89**, 5547–5551.
6. Wang, Y., O'Malley, B. W., Jr., Tsai, S. Y. & O'Malley, B. W. (1994) *Proc. Natl. Acad. Sci. USA* **91**, 8180–8184.
7. Yu, S.-F., von Rueden, T., Kantoff, P. W., Garber, C., Seiberg, M., Ruether, U., Anderson, W. F., Wagner, E. F. & Gilboa, E. (1986) *Proc. Natl. Acad. Sci. USA* **83**, 3194–3198.
8. Jackson, R. J., Howell, M. T. & Kaminski, M. (1990) *Trends Biochem. Sci* **15**, 477–483.
9. Sambrook, J., Fritsch, E. F. & Maniatis, T. (1989) *Molecular Cloning: A Laboratory Manual* (Cold Spring Harbor Lab. Press, Plainview, NY), 2nd Ed.
10. Morgenstern, J. P. & Land, H. (1990) *Nucleic Acids Res.* **18**, 3587–3596.
11. Rando, T. A. & Blau, H. M. (1994) *J. Cell Biol.* **125**, 1275–1287.
12. Sanes, J. R., Rubenstein, J. L. & Nicolas, J. F. (1986) *EMBO J.* **5**, 3133–3142.
13. Nolan, G. P., Fiering, S., Nicolas, J.-F. & Herzenberg, L. A. (1988) *Proc. Natl. Acad. Sci. USA* **85**, 2603–2607.
14. Pear, W. S., Nolan, G. P., Scott, M. L. & Baltimore, D. (1993) *Proc. Natl. Acad. Sci. USA* **90**, 8392–8396.
15. Spicher, A., Etter, A., Bernard, V., Tobler, H. & Mueller, F. (1994) *Dev. Biol.* **164**, 72–86.
16. Gossen, M., Freundlieb, S., Bender, G., Mueller, G., Hillen, W. & Bujard, H. (1995) *Science* **268**, 1766–1769.
17. Figge, J., Wright, C., Collins, C. J., Roberts, T. M. & Livingston, D. M. (1988) *Cell* **52**, 713–722.
18. Chalfie, M., Tu, Y., Euskirchen, G., Ward, W. W. & Prasher, D. C. (1994) *Science* **263**, 802–805.
19. Dhawan, J., Rando, T. A., Elson, S. L., Bujard, H. & Blau, H. M. (1995) *Somatic Cell Mol. Genet.* **21**, 233–240.
20. Shockett, P., Difilippantonio, M., Hellman, N. & Schatz, D. G. (1995) *Proc. Natl. Acad. Sci USA* **92**, 6522–6526.
21. Furth, P. A., Onge, L. S., Boeger, H., Gruss, P., Gossen, M., Kistner, A., Bujard, H. & Hennighausen, L. (1994) *Proc. Natl. Acad. Sci. USA* **91**, 9302–9306.

EXHIBIT D

JOURNAL OF VIROLOGY, Apr. 1988, p. 1120–1124
0022-538X/88/041120-05$02.00/0

Vol. 62, No. 4

A Safe Packaging Line for Gene Transfer: Separating Viral Genes on Two Different Plasmids

DINA MARKOWITZ,[1] STEPHEN GOFF,[2] AND ARTHUR BANK[1,3]*

Department of Genetics and Development,[1] Department of Biochemistry and Molecular Biophysics,[2] and Department of Medicine,[3] College of Physicians and Surgeons, Columbia University, New York, New York 10032

Received 19 May 1987/Accepted 14 December 1987

A retrovirus packaging cell line was constructed by using portions of the Moloney murine leukemia virus in which the *gag*, *pol*, and *env* genes of the helper virus were separated onto two different plasmids and in which the ψ packaging signal and 3′ long terminal repeat were removed. The plasmid containing the *gag* and *pol* genes and the plasmid containing the *env* gene were cotransfected into NIH 3T3 cells. Clones that produced high levels of reverse transcriptase and *env* protein were tested for their ability to package the replication-defective retrovirus vectors Δneo and N2. One of the *gag-pol* and *env* clones (GP+E-86) was able to transfer G418 resistance to recipient cells at a titer of as high as 1.7×10^5 when it was used to package Δneo and as high as 4×10^6 when it was used to package N2. Supernatants of clones transfected with the intact parent *gag-pol-env* plasmid 3P0 had comparable titers (as high as 6.5×10^4 with Δneo; as high as 1.7×10^5 with N2). Tests for recombination events that might result in intact retrovirus showed no evidence for the generation of replication-competent virus. These results suggest that *gag*, *pol*, and *env*, when present on different plasmids, may provide an efficient and safe packaging line for use in retroviral gene transfer.

The cloning, transfer, and expression of human globin genes into erythroid cells in culture and in mice has raised the possibility of autotransplantation of bone marrow cells with a normal β-globin gene as an approach to therapy of sickle cell anemia and β-thalassemia in humans (5). Retroviral vectors are the most efficient means of transferring genes into cells. This high efficiency is a requirement for experiments whose goal is human globin gene therapy since only a limited number of bone marrow stem cells can be obtained, and as many cells as possible must acquire and express the transferred genes to ensure repopulation of sufficient bone marrow elements to produce normal amounts of hemoglobin. Another major prerequisite in these experiments is safety (1). The major danger of the use of retroviral vectors is the possibility that replication-competent viruses could form and that the proliferation of those viruses would lead to multiple integrations into the genome. Those integrations could result in activation of potentially harmful genes such as oncogenes (21, 24) and could lead to other harmful consequences of their proliferation. To avoid these complications, packaging lines have been constructed in which the retroviral sequences in the helper virus are not by themselves transmissible, replication-competent viruses (4, 15, 18, 23, 25). In these defective viral constructs, the signal for packaging of viral RNA (ψ sequence) has been deleted. Thus, while the required *gag*, *pol*, and *env* genes of the retrovirus are intact, there is no release of wild-type helper virus by these packaging lines. However, when the ψ packaging lines are transfected with replication-defective retroviral vectors containing an intact ψ sequence required for their own packaging, wild-type retrovirus can arise, presumably by recombination events (15). For example, high-titer amphotropic retroviral stocks generated by the transfer of a defective neomycin-containing retrovirus into the amphotropic packaging cell line PA12 (containing the ψ deletion) have been shown to produce infectious amphotropic helper virus (11, 16). To circumvent this problem, additional mutations have been made in the defective virus of newer helper cell lines (2, 16). These have included deletions in the 3′ long terminal repeat (LTR) of the helper virus component, and additional deletions of portions of the 5′ LTR as well. One of these defective amphotropic constructs was used to produce a retroviral packaging line, PA317, that has recently been reported to eliminate wild-type retrovirus production after retroviral transfection. However, by use of this packaging line, two recombinational events could still produce intact retrovirus. Cell lines containing both 3′ and 5′ LTR deletions and the packaging mutation were also constructed but were not useful because of the relatively low titers obtained with these constructs.

We approached this problem by attempting to create a packaging cell line by using helper virus DNA in which the *gag* and *pol* genes were on one plasmid while the *env* gene was on another. In addition, the two plasmids had deletions of the ψ packaging sequence and the 3′ LTRs. A stable and efficient packaging line was created by using these two plasmids, and as predicted, the three recombinational events necessary to lead to the production of intact retrovirus could not be detected. Thus, this approach satisfies the requirement for human gene therapy that the use of retroviral vectors must involve, as close as possible, completely safe retroviral packaging lines and must permit efficient gene transfer into recipient cells.

MATERIALS AND METHODS

Helper virus genomic construction. By using the Moloney murine leukemia virus (Mo-MULV) present in the plasmid 3P0 as the starting material (Fig. 1), two constructions were made: (i) p*gag-pol*gpt, containing the *gag* and *pol* genes of Mo-MULV; and (ii) p*env*, containing the *env* gene from this virus (Fig. 1).

p*gag-pol*gpt. p*gag-pol*gpt (Fig. 2) was constructed by using the plasmid pSV2gpt (20) as the source of simian virus 40 sequences and the *gpt* gene as the selectable marker. The plasmid 3P0 contains Mo-MULV proviral DNA with a 134-base-pair deletion of the ψ packaging signal, from *Ba*I at

* Corresponding author.

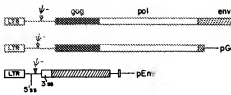

FIG. 1. Comparison of viral sequences contained in parent plasmid 3P0 and constructs p*gag-pol*gpt and p*env*. Mo-MULV LTRs and the ψ deletion (ψ^-) are indicated. Symbols and abbreviations: solid regions, *gag* sequences; open regions, *pol* sequences; hatched regions, *env* sequences; solid lines, nontranslated viral sequences; 5′ ss, 5′ splice donor; 3′ ss, 3′ splice acceptor.

position 660 to *Xma*III at position 794 (L. Lobel and S. Goff, personal communication). 3P0 DNA was digested with *Sca*I and *Nae*I, both of which left blunt ends; and a 7.9-kilobase (kb) fragment containing the 5′ LTR and the *gag* and *pol* genes was isolated from a 1.7% agarose gel by electroelution. Plasmid pSV2gpt was digested at its unique *Bam*HI site, and its protruding 5′ ends were filled in by using the Klenow fragment of DNA polymerase and all four deoxynucleoside triphosphates. The 7.9-kb *gag-pol* fragment was then ligated to the blunt-ended 5.1-kb pSV2gpt vector, and positive colonies were isolated by using colony filter hybridization (10) and probing with a nick-translated 2.54-kb *Bgl*II fragment from 3P0 (*gag-pol* probe). DNAs from individual colonies were then tested for the correct orientation of the *gag-pol* insert by digesting them with *Eco*KI. The resulting 13.4-kb plasmid was named p*gag-pol*gpt (Fig. 2).

p*env*. Plasmid 3P0 was digested with *Bgl*II and *Nhe*I (Fig. 2). The 2.4-kb *env* fragment at positions 5858 to 8297

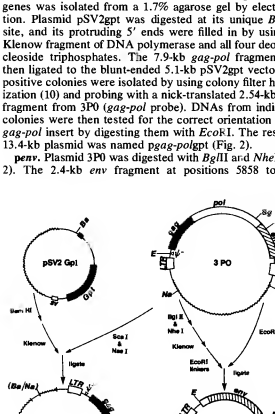

FIG. 2. Schematic diagram showing construction of plasmids p*gag-pol*gpt and p*env*. Symbols and abbreviations: wavy lines, pBR322 sequences; thin lines, plasmid sequences; small solid box, simian virus 40 poly(A) sequence; SV, simian virus 40 origin of replication; ψ^-, deletion of ψ packaging sequences; Ba, *Bam*HI; Bg, *Bgl*II; E, *Eco*RI; Na, *Nae*I; Nh, *Nhe*I; S, *Sca*I.

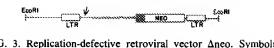

FIG. 3. Replication-defective retroviral vector Δneo. Symbols and abbreviations: ψ, packaging sequence; wavy line, pBR322 sequences; solid box, simian virus 40 promoter and origin of replication.

containing the 3′ acceptor splice site was isolated by electroelution from a 1.2% agarose gel. The ends were filled in with the Klenow fragment of DNA polymerase and all four deoxynucleoside triphosphates, and *Eco*RI linkers were ligated to both ends. The 5′ LTR and 5′ donor splice site were prepared by digesting 3P0 DNA with *Eco*RI and isolating the 6.2-kb fragment by electroelution from a 1% agarose gel. The 6.2-kb fragment was treated with phosphatase and then ligated to the 2.4-kb *env* fragment. Positive transformants were isolated by using the colony filter hybridization technique, probed with a labeled 1.3-kb *Hpa*I fragment from 3P0 (*env* probe). DNAs from positive colonies were then tested for the correct orientation of the *env* insert by digesting them with either *Xba*I or *Sca*I. The resulting 8.6-kb plasmid was named p*env* (Fig. 2).

Electroporation and cell analysis. NIH 3T3 cells were transfected with p*gag-pol*gpt or the p*env* plasmid by electroporation (22). For each experiment, 10^7 cells were collected by centrifugation and suspended in 0.5 ml of sterile, 1× phosphate-buffered saline. The cells were then mixed with 10 μg of nonselectable plasmid DNA and 5 μg of selectable plasmid DNA or with 5 μg of selectable plasmid DNA alone. The cell-DNA suspension was loaded into a 0.5-ml electroporation chamber (model ZA1000; Prototype Design Services, Madison, Wis.) and a bank of capacitors (effective capacity, 14 μF), charged to 500 to 1,000 V, and discharged via an electronic switch through the solution. The cells were then suspended in 100 ml of Dulbecco modified Eagle medium, supplemented with 10% newborn calf serum–penicillin (100 μg/ml)–streptomycin (100 μg/ml)–amphotericin B (0.25 μg/ml), and plated in four 24-well plates. Selective medium was added 48 to 72 h after the electroporation.

The plasmids p*gag-pol*gpt and p*env* were coelectroporated into NIH 3T3 cells; as a control, 3P0 and pSV2gpt were also coelectroporated into NIH 3T3 cells. Cells were selected for the presence of the *gpt* gene with medium containing 15 μg of hypoxanthine per ml, 250 μg of xanthine per ml, and 25 μg of mycophenolic acid (MA) per ml (HXM medium). Clones selected with HXM medium were then analyzed for reverse transcriptase (RT) production as described previously (8). Positive controls for RT activity were ψ2 cell (15) supernatants and supernatants from wild-type Mo-MULV clone 4 cells. Negative controls for RT activity were untransfected NIH 3T3 supernatants and RT cocktail alone.

Packaging lines were transfected with the retroviral vector plasmids Δneo and N2 by electroporation of 10^7 NIH 3T3 cells with 5 μg of plasmid DNA. Both plasmids contain a neomycin resistance (*neo*^{r}) gene; eucaryotic cells expressing the gene were selected with the antibiotic G418 (800 μg/ml). Δneo is a 6.6-kb replication-defective retroviral plasmid in which the *neo*^{r} gene is flanked by intact LTRs and has 5′ *gag* sequences, including an intact ψ sequence (Fig. 3) (14a); N2 has been described previously (12).

Analysis of viral proteins. The presence and expression of p*env* was analyzed by metabolic labeling and immunoprecipitation of gPr80*env*, the *env* protein, with *env* antiserum as follows. Clones of confluent cells (on 10-cm-diameter plates) were starved for 20 min in Dulbecco modified Eagle

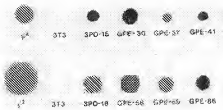

FIG. 4. RT assays of supernatants from clones of cells transfected with 3P0 or cotransfected with *pgag-pol*gpt and *penv*. Individual clones resistant to MA were isolated, and the supernatant fluid was assayed for RT on an exogenous template (8). Results are shown from two different experiments (top and bottom lines). Included in each experiment are positive (ψ^2 supernatant) and negative (NIH 3T3 supernatant) controls.

medium minus methionine, and 150 μCi of [^{35}S]methionine (Amersham Corp. Arlington Heights, Ill.) was added for 40 min. The cells were lysed in 1% Triton X-100–0.5% deoxycholate–0.1% sodium dodecyl sulfate–10 mM sodium phosphate (pH 7.5)–0.1 M NaCl; the cell lysate was spun down in a T150 or T180 rotor at 35,000 × *g* for 3 h at 4°C. The supernatant was incubated with normal goat serum, and nonspecifically bound proteins were precipitated with pansorbin (staph A protein; Calbiochem-Behring, La Jolla, Calif.). The remaining supernatant was incubated with *env* antiserum (795-771; National Cancer Institute, Rockville, Md.) overnight, and the immunoprecipitates were collected with pansorbin. The labeled proteins were analyzed by electrophoresis on a sodium dodecyl sulfate–10% polyacrylamide gel (13), followed by fluorography.

Virus production. Titers of CFU were determined by infection of NIH 3T3 cells with dilutions of the viral harvest as follows. NIH 3T3 cells (5×10^5) were seeded in a 6-cm-diameter petri dish. Eighteen hours later the viral harvest supernatants from clones of semiconfluent cells were filtered through 0.45-μm-pore-size filters (Millipore Corp., Bedford, Mass.), and 1 ml was applied to the cells. Polybrene (8 μg/ml; dextran) was added to the supernatants to enhance the titer. After 2 h at 37°C, 4 ml of medium was added to the cells; 48 h later the cells were trypsinized and plated onto a 10-cm-diameter plate in medium containing 800 μg of G418 per ml; 10 to 14 days later clones were counted.

RESULTS

Generation of the packaging line. To generate cell lines expressing *gag-pol* and *env* regions from different plasmids, NIH 3T3 cells were cotransfected with p*gag-pol*gpt and p*env* DNAs. Recipient cells were then selected with medium containing MA. Eighty-six MA-resistant (GP+E) clones were isolated, and their supernatants were tested for RT. Twenty-seven clones were found to produce a high level of RT (Fig. 4). In a separate electroporation, 3P0 DNA, containing an intact set of *gag*, *pol*, and *env* genes, was coelectroporated with pSV2gpt into NIH 3T3 cells. Of 16 MA-resistant clones obtained from this electroporation and tested, supernatants from 3 were high in RT (Fig. 4). The RT levels of the high RT-producing GP+E clones were equal to those of the high RT-producing 3P0 clones.

Twenty-one of the high RT-producing GP+E clones were then analyzed for *env* protein expression by metabolic labeling, followed by immunoprecipitation with *env* antiserum. A total of 11 of the clones were positive for gPr80*env*; 3 clones produced a strong signal, 4 produced a medium signal, and 4 produced a weak signal (Fig. 5).

Ability of cell lines to package retroviral vectors. To test the packaging ability of cell lines containing a fragmented retroviral genome, five GP+E clones that expressed high levels of RT and medium to high levels of *env* were transfected with Δneo DNA, and recipient cells were selected with G418 as described above. A number of G418-resistant clones (GP+E+Δneo) were collected from each transfected GP+E cell line.

To determine viral titers, supernatants from GP+E+Δneo clones were filtered, and a 1-ml portion of undiluted or diluted supernatant was used to infect NIH 3T3 cells as described above. The titers of the GP+E+Δneo clones ranged from 1×10^2 to 1.7×10^5 CFU/ml (Table 1). Supernatants from G418-resistant clones assayed for Δneo virus titers in the *gag-pol-env* packaging clone 3P0-18 pro-

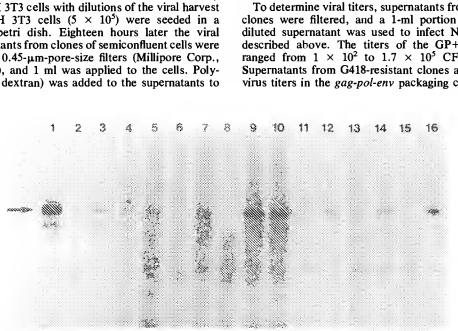

FIG. 5. Analysis of viral *env* protein synthesis in transfected NIH 3T3 cells. Plasmids p*gag-pol*gpt and p*env* were cotransfected into NIH 3T3 cells. Individual clones resistant to MA and which expressed high levels of RT were labeled with [^{35}S]methionine. The labeled proteins were analyzed by immunoprecipitation, sodium dodecyl sulfate-polyacrylamide gel electrophoresis, and fluorography, as described in the text. Lane 1, Proteins from 3P0-18 cells; lanes 2 to 16, proteins from GP+E clones 5, 21, 30, 37, 38, 41, 42, 43, 46, 56, 58, 66, 69, 75, and 86, respectively. The position of protein gPr80^{env} is indicated by the arrow.

TABLE 1. Virus production from packaging cells containing retroviral vectors

Packaging cell line	Vector	Clone	Titer (CFU/ml)	Secondary titer (CFU/ml)[a]	Secondary RT[b]
GP+E-86	Δneo	1	1.25×10^3	0	–
		8	3×10^4	0	–
		11	9×10^4	0	–
		17	6.5×10^4	0	–
		21	1.7×10^3	0	–
ψ2	Δneo	4	4.6×10^4		
		6	5.4×10^4		
3P0-18	Δneo	1	2.2×10^4	0	
		2	1.1×10^4		
		3	5.7×10^3		
		4	8×10^2		
		5	6.7×10^3	0	
		7	6.5×10^4	0	
GP+E-86	N2	3	1.23×10^6		
		7	3.5×10^6		
		8	2.6×10^6		
		9	3×10^6		
		11	1.33×10^6		
		12	4×10^6		
		13	3.6×10^6		
		17	2.5×10^6		
		20	1.34×10^6		
		22	3×10^6		
3P0-18	N2	1	3.75×10^4		
		2	1.85×10^4		
		3	4×10^4		
		6	10^5		
		9	6×10^4		
		10	10^5		
		11	1.7×10^5		

[a] Supernatants from pools of G418-resistant Δneo virus-infected NIH 3T3 cells were analyzed for the Δneo virus titer.
[b] Supernatants from pools of G418-resistant Δneo virus-infected NIH 3T3 cells were assayed for RT as described in the text.

duced titers from 8×10^2 to 6.5×10^4 CFU/ml. The titer of Δneo released from ψ2 cells was 4.6×10^4 to 5.4×10^4 CFU/ml. The GP+E-86 packaging line produced consistently higher titers than the other four packaging lines, and was therefore used in subsequent experiments.

GP+E-86 cells were also tested for their ability to package the retroviral vector N2. N2 DNA was electroporated into GP+E-86 cells, and 22 G418-resistant clones (GP+E+N2) were isolated. N2 viral titers from GP+E+N2 clones ranged from 5.3×10^5 to 4×10^6 CFU/ml, with 17 of 22 (77%) clones generating titers of $>10^5$ CFU/ml. Titers from clones of 3P0−18 cells transfected with N2 ranged from $<1 \times 10^2$ to 1.7×10^5 CFU/ml, with 5 of 11 (45%) generating titers of $>1 \times 10^5$ CFU/ml.

Analysis for recombinant infectious retrovirus. As a preliminary test for infectious retrovirus, supernatants from five high-titer GP+E+Δneo clones were used to infect NIH 3T3 cells. The infected NIH 3T3 cells were selected with G418 and allowed to develop into a confluent layer of G418-resistant clones. Supernatants from these plates (secondary GP+E+Δneo supernatants) were then used to infect fresh NIH 3T3 cells. These NIH 3T3 cells were again selected with G418, resulting in no surviving G418-resistant cells. These same supernatants also tested negative for RT. These results indicate that there is no viral rescue of Δneo from the initial NIH 3T3 cells infected with GP+E+Δneo primary supernatants.

In a more stringent test for infectious retrovirus, NIH 3T3 cells were infected with supernatants from high-titer GP+E+Δneo clones. The infected NIH 3T3 cells were passaged continuously for 1 month without G418 selection. This treatment would have allowed the spread of a rare recombinant wild-type virus throughout the population of cells and, therefore, the spread of infectious Δneo particles into originally noninfected NIH 3T3 cells (that would have been killed off had the cells been exposed to G418). After 1 month in culture, supernatants were tested for Δneo production by infecting fresh NIH 3T3 cells and testing them for G418 resistance. As in the previous experiment, no G418-resistant cells were obtained.

In a third test for the safety of the GP+E-86 packaging line, we designed an experiment that could detect a transfer of packaging function. NIH 3T3 cells were electroporated with N2 DNA, and pools of G418-resistant clones (NIH 3T3-N2 pools) were collected. Supernatant medium from GP+E-86 cells was used to infect the NIH 3T3-N2 pools. If the NIH 3T3-N2 pools became infected with the wild-type virus secreted from GP+E-86 cells, resulting in a transfer of packaging function, these cells would begin to secrete N2 virus. The supernatant from the infected NIH 3T3-N2 pools was harvested and used to infect NIH 3T3 cells. These NIH 3T3 cells were then assayed for the presence of N2 virus by exposing the cells to G418. Using this type of assay, we were unable to detect G418-resistant colony production; therefore, GP+E-86 cells are unable to transfer the packaging function, as demonstrated by an inability to rescue N2 virus from NIH 3T3 cells.

DISCUSSION

A safe packaging line essentially incapable of permitting recombinational events that can result in an intact infectious retroviral genome is a requirement for the use of retroviral vectors in human gene therapy. While recently used vector systems are relatively safe, their design is flawed by the potential for two recombination events resulting in the generation of infectious retrovirus. In the experiments described here, we separated portions of the helper virus genome so that the generation of an intact retroviral genome would be extraordinarily unlikely, if not impossible. We separated the *gag* and *pol* genes on one plasmid and the *env* gene on another plasmid. In addition, we kept the packaging (ψ) mutation in both of these plasmids and eliminated the 3′ LTR, thus, further diminishing the opportunity for recombination. We demonstrated that the fragmented helper virus genome, when introduced into NIH 3T3 cells, appears to produce titers of retroviral particles comparable to those of the intact Mo-MULV helper from which the components were derived. Analysis of NIH 3T3 cells transfected with these fragmented genomes has been simplified by the availability of a sensitive RT assay (8) to detect *gag-pol* expression and a sensitive *env* assay to measure the expression of this important gene.

We obtained an optimal packaging line (GP+E-86) that produces high *gag-pol* and *env* protein levels, as demonstrated by the RT assay and immunoprecipitation with *env* antiserum. GP+E-86 cells (which contain *gag* and *pol* on one plasmid and *env* on another plasmid), on transfection with the retroviral vectors Δneo and N2, released titers that were comparable to those released by 3P0-18 and ψ2 cells

(which contain an intact *gag-pol-env* plasmid). The titers that were obtained were comparable to those reported by other investigators who used defective retrovirus (2, 4, 5, 15, 16, 18, 23, 25) and were high enough for use in gene transfer experiments in animals (3, 6, 7, 9, 11, 14, 17, 26, 27).

Thus far, we have found no evidence for recombinational events occurring when *gag-pol* on one plasmid and *env* on another are used in plasmids that also contain ψ mutations and deletions of 3' LTRs. Cells that were electroporated with these packaging plasmids and then with vector plasmids did not appear to produce the three recombination events needed for the generation of wild-type virus. Thus, this packaging line may be especially safe for use in experiments whose goal is human gene therapy. We are currently preparing a similar amphotropic packaging line for this purpose.

ACKNOWLEDGMENTS

We thank Norma Lerner for providing the Aneo plasmid, Leslie Lobel for providing the 3P0 plasmid, Eli Gilboa for providing the N2 plasmid, and Oona Collins for editorial assistance.

This study was supported by Public Health Service grants DK-25274, HL-37069, and HL-07230 from the National Institutes of Health and by the March of Dimes Birth Defects Foundation.

LITERATURE CITED

1. **Anderson, W. F.** 1984. Prospects for human gene therapy. Science **226**:401–409.
2. **Bassetman, R. A., R. Hu, J. Bruszewski, S. Hu, F. Martin, and M. Nicolson.** 1987. Replication-defective chimeric helper proviruses and factors affecting generation of competent virus: expression of Moloney murine leukemia virus structural genes via the metallothionein promoter. Mol. Cell. Biol. **7**:1797–1806.
3. **Cline, M. J., H. Stang, K. Mercola, L. Morse, R. Ruprecht, J. Browne, and W. Salser.** 1980. Gene transfer in intact animals. Nature (London) **284**:422–425.
4. **Cone, R. D., and R. C. Mulligan.** 1984. High efficiency gene transfer into mammalian cells: generation of helper-free retrovirus with broad mammalian host range. Proc. Natl. Acad. Sci. USA **81**:6349–6353.
5. **Cone, R. D., A. Weber-Benarous, D. Baorto, and R. C. Mulligan.** 1987. Regulated expression of a complete human β-globin gene encoded by a transmissible retrovirus vector. Mol. Cell. Biol. **7**:887–897.
6. **Dick, J. E., M. C. Magli, D. Huszar, R. A. Phillips, and A. Bernstein.** 1985. Introduction of a selectable gene into primitive stem cells capable of long-term reconstitution of the hemopoietic system of W/W^V mice. Cell **42**:71–79.
7. **Eglitis, M. A., P. Kantoff, E. Gilboa, and W. F. Anderson.** 1985. Gene expression in mice after high efficiency retroviral-mediated gene transfer. Science **230**:1395–1398.
8. **Goff, S. P., P. Traktman, and D. Baltimore.** 1981. Isolation and properties of Moloney murine leukemia virus mutants: use of a rapid assay for release of virion reverse transcriptase. J. Virol. **38**:239–248.
9. **Gruber, H. E., K. D. Finley, R. M. Hershberg, S. S. Katzman, P. K. Lalkind, J. E. Seegmiller, T. Friedman, J. Yee, and D. J. Jolly.** 1985. Retroviral vector-mediated gene transfer into human hematopoietic progenitor cells. Science **230**:1057–1060.
10. **Grunstein, M., and D. S. Hogness.** 1975. Colony hybridization: a method for isolation of cloned DNAs that contain a specific gene. Proc. Natl. Acad. Sci. USA **72**:3961–3965.
11. **Hock, R. A., and A. D. Miller.** 1986. Retrovirus-mediated transfer and expression of drug-resistant genes in human haematopoietic progenitor cells. Nature (London) **320**:275–277.
12. **Keller, G., C. Paige, E. Gilboa, and E. F. Wagner.** 1985. Expression of a foreign gene in myeloid and lymphoid cells derived from multipotent haematopoietic precursors. Nature (London) **318**:149–154.
13. **Laemmli, U. K.** 1970. Cleavage of structural proteins during the assembly of the head of bacteriophage T4. Nature (London) **227**:680–685.
14. **Lemischka, I. R., D. H. Raulet, and R. C. Mulligan.** 1986. Developmental potential and dynamic behavior of hematopoietic stem cells. Cell **45**:917–927.
14a. **Lerner, N., S. Brigham, S. Goff, and A. Bank.** 1987. Human β-globin gene expression after gene transfer using retroviral vectors. DNA **6**:573–582.
15. **Mann, R., R. C. Mulligan, and D. Baltimore.** 1983. Construction of a retrovirus packaging mutant and its use to produce helper-free defective retrovirus. Cell **33**:153–159.
16. **Miller, A. D., and C. Buttimore.** 1986. Redesign of retrovirus packaging cell lines to avoid recombination leading to helper virus production. Mol. Cell. Biol. **6**:2895–2902.
17. **Miller, A. D., R. J. Eckner, D. J. Jolly, T. Friedman, and I. M. Verma.** 1984. Expression of a retrovirus encoding human HPRT in mice. Science **225**:630–632.
18. **Miller, A. D., M.-F. Law, and I. M. Verma.** 1985. Generation of helper-free amphotropic retroviruses that transduce a dominant-acting methotrexate-resistant dihydrofolate reductase gene. Mol. Cell. Biol. **5**:431–437.
19. **Mulligan, R. C., and P. Berg.** 1980. Expression of a bacterial gene in mammalian cells. Science **209**:175–183.
20. **Mulligan, R. C., and P. Berg.** 1981. Selection for animal cells that express the *Escherichia coli* gene coding for xanthine-guanine phosphoribosyltransferase. Proc. Natl. Acad. Sci. USA **78**:2072–2076.
21. **Neel, B. G., W. S. Hayward, H. L. Robinson, J. Fang, and S. M. Astrin.** 1981. Avian leukosis virus-induced tumors have common proviral integration sites and synthesize discrete new RNAs: oncogenesis by promoter insertion. Cell **23**:323–334.
22. **Potter, H., L. W. Weir, and P. Leder.** 1984. Enhancer-dependent expression of human K immunoglobulin genes introduced into mouse pre-B lymphocytes by electroporation. Proc. Natl. Acad. Sci. USA **81**:7161–7165.
23. **Sorge, J., D. Wright, V. D. Erdman, and A. Cutting.** 1984. Amphotropic retrovirus system for human cell gene transfer. Mol. Cell. Biol. **4**:1730–1737.
24. **Varmus, H. E., N. Quintrell, and S. Ortiz.** 1981. Retroviruses as mutagens: insertion and excision of a nontransforming provirus alter expression of a resident transforming provirus. Cell **25**:23–36.
25. **Watanabe, S., and H. M. Temin.** 1983. Construction of a helper cell line for avian reticuloendotheliosis virus cloning vectors. Mol. Cell. Biol. **3**:2241–2249.
26. **Williams, D. A., I. R. Lemischka, D. G. Nathan, and R. C. Mulligan.** 1984. Introduction of new genetic material into pluripotent haematopoietic stem cells of the mouse. Nature (London) **310**:476–480.
27. **Williams, D. A., S. H. Orkin, and R. C. Mulligan.** 1986. Retrovirus-mediated transfer of human adenosine deaminase gene sequences into cells in culture and into murine hematopoietic cells *in vivo*. Proc. Natl. Acad. Sci. USA **83**:2566–2570.